

20 July 1977

BEAM TRANSPORT POSSIBILITIES OF THE LOW ENERGY BEAM TRANSPORT SYSTEM

(LEBT) OF THE NEW 50 MEV LINAC

K. Crandall ^{*)} and M. Weiss

SUMMARY

The LEBT of the new 50 MeV Linac is analysed with respect to its capability of transporting pre-injector beams of different intensities and emittances ; the situation in the transverse phase space is of main concern.

Some formulae showing general features of triplet focusing are derived ; they are useful for the design and assessment of limitations of a beam transport system. The LEBT acceptance is also calculated and the limitations indicated ; in this respect, a general focusing diagram is presented, which, by appropriate scaling remains valid for all beams.

For the operation of LEBT, a procedure of setting the focusing parameters is described ; it makes use of the existing beam measuring possibilities and of the on-line beam transport program TRACE. Some examples are given.

*) Visiting scientist from LASL, Los Alamos, USA.

I N D E X

1. INTRODUCTION
2. GENERAL FEATURES OF QUADRUPOLE TRIPLETS
3. ACCEPTANCE OF LEBT AND FOCUSING CONSIDERATIONS
4. POSSIBILITIES OF REMOVING LEBT ACCEPTANCE LIMITATIONS
5. PROCEDURE FOR THE ADJUSTMENT OF FOCUSING PARAMETERS
6. OPERATION OF LEBT - Final state
7. CONCLUSION

1. INTRODUCTION

The purpose of this paper is the analysis of LEBT ¹⁾ in order to determine the range of preinjector beams which can be conveniently transported and matched to the Linac input. In a certain sense, this task is equivalent to the calculation of the LEBT acceptance and the recognition of its limitations.

The problem has been approached along two lines : an analytical, where general formulae were established giving a good insight into essential features of triplet focusing (the first focusing elements in LEBT are quadrupole triplets) ; the other numerical, where the on-line program TRACE ²⁾ was used to compute the actual LEBT acceptance and the corresponding triplet settings. Here it was possible to establish a general acceptance and focusing diagram, which, with an appropriate scaling remained valid for all beams (provided the beam transport is space charge dominated). The actual limitations on the LEBT acceptance could eventually be removed, to a certain extent, if the need arises ; the modifications to be undertaken are briefly outlined.

The operational aspects of LEBT are also dealt with in this paper. It is shown how the focusing parameters can be approximately set in a controllable way, making a combined use of beam measuring facilities and of the on-line program TRACE.

The matching in the longitudinal plane is not treated in this paper.

2. GENERAL FEATURES OF QUADRUPOLE TRIPLETS

In beam transport systems using triplets, the basic two questions to be answered are :

- a) what is the required focusing strength of the triplet ;
- b) what is the permissible distance between triplets.

2.a) Triplets are usually used in systems where one wishes to transport rotationally symmetric beams ; the focusing in both transverse planes is then equal. Under such a condition, the maximum focusing strength, Δ_{\max} , one can in principle obtain from a symmetric triplet depends on the size of it ; as derived in Appendix 1, the expression holds

$$\Delta_{\max} \cdot \ell = \text{const.} \cong 0.34 , \quad (2.1)$$

where ℓ is the distance between centres of adjacent quadrupoles, see Fig. 1a. In other words, if high Δ_{\max} are required, ℓ is to be kept low, which means that short quadrupoles have to be used. This is just the opposite of what one would at first be tempted to proceed.

Short quadrupoles have a higher percentage of end aberrations ; hence a compromise must be reached in the choice of triplets, taking aberrations and the margin in focusing strength into account.

2.b) To transport a beam of a given size, the distance between focusing elements must be well chosen ; if this distance exceeds a certain value, it can happen that no matching solutions exist any more.

The problem has been analyzed in Appendix 2 on a model consisting of two triplets spaced by a distance L (centre to centre) ; see also Fig. 2a. In the absence of space charge, matching solutions exist if

$$L \leq \sqrt{\beta_1 \beta_2} , \quad (2.2)$$

where β_1 and β_2 are the Twiss parameters of the beam at the first and second triplet respectively.

With space charge, this expression is modified ; using the model of Fig. 2b, one obtains the condition :

$$L \left(1 + \frac{\Delta_{sc} L}{4} \right) \leq \sqrt{\beta_1 \beta_2} \quad \text{or} \quad L \leq \frac{2}{\Delta_{sc}} \left(\sqrt{1 + \Delta_{sc} \sqrt{\beta_1 \beta_2}} - 1 \right) , \quad (2.3)$$

where Δ_{sc} represents the defocusing "space charge lens",

$$\Delta_{sc} [m^{-1}] \cong \frac{eIL}{2\pi\epsilon_0 m v^3 \hat{r}_{av}^2} , \quad (2.4)$$

I being the beam intensity and \hat{r}_{av}^2 the square of an average beam radius over the distance L .

Formulae (2.3) are very useful in judging if a beam of a given size can be transported over a distance L ; or, vice versa, given the distance L , one can find the corresponding minimum beam sizes, which are still allowed.

The analytic treatment outlined in 2.a) and 2.b) is useful in pointing to the essential properties of triplet focusing and in assessing transfer capabilities to a beam transport system even before one starts with detailed numerical calculations. It indicates also what is to be undertaken in concrete cases in order to eventually remove some acceptance limitations.

3. ACCEPTANCE OF LEBT AND FOCUSING CONSIDERATIONS

In Fig. 3 LEBT is presented schematically ; the focusing in the unbunched beam part consists of four symmetric triplets. After the second triplet follows a system of four-jaw apertures, AP1 and AP2 ; by conditions imposed at AP1, the beam can be limited proportionally in divergence and diameter. The third and the fourth triplets (T3, T4) serve to match the beam to the buncher DDHB (double drift harmonic buncher). Once the beam has been correctly transferred to AP1, beam transport computations show that it can then also be matched to the buncher. The "critical" part of LEBT thus remains the part up to AP1, containing the triplets T1 and T2.

Prior to the acceptance calculation, it will be shown that the focusing in LEBT is space charge dominated. From the smooth envelope equation (the symbols have the usual meaning, see e.g. ⁴⁾) :

$$\hat{x}'' = K\hat{x} - \frac{E^2}{\hat{x}^3} - \frac{kI}{\hat{x}} = 0 \quad (3.1)$$

and by putting the matched beam condition : $\hat{x} = 0$, one obtains :

$$K = \frac{E^2}{\hat{x}^4} \left(1 + \frac{kI\hat{x}^2}{E^2} \right) = \frac{1}{\beta^2} \left(1 + k\beta \frac{I}{E} \right) = K_0 (1 + \sigma) \quad (3.2)$$

K_0 is the smooth focusing without space charge, σ is the dimensionless space charge parameter and β is the amplitude function. A convenient formula for σ is the following :

$$\sigma \cong \beta[m] \frac{I[mA]}{E[mm \text{ mrad}]} ; \quad (3.3)$$

with these units, $k = 1$.

Taking, as example, the usual beams in LEBT one gets :

$$\left. \begin{aligned} I &= 200 \text{ mA} \\ E &= 50 \text{ mm mrad} \\ \beta &= 3\text{m} (\hat{x} \cong 12.5 \text{ mm}) \end{aligned} \right\} \sigma = 12$$

As $\sigma \gg 1$, the focusing in LEBT is strongly space charge dominated and formula (3.2) becomes :

$$K \cong K_0 \sigma \cong \frac{1}{\beta} [\text{m}^{-1}] \frac{I[\text{mA}]}{E[\text{mm mrad}]} . \quad (3.4)$$

The focusing depends on the ratio I/E (in what follows this ratio will always be quoted in above units) and inversely on β . Beams with different I/E can be transported with the same focusing, provided β is changed accordingly (I/\hat{x}^2 is to be kept constant).

In Fig. 4 are shown the conditions one imposes on the beam at AP1 ; they are a function of the ratio I/E only (see also ¹⁾). With these conditions and using TRACE, one has explored the range of input beams which can be accepted by LEBT.

At first one has calculated a set of quadrupole strengths for triplets T1 and T2 that produced a match at AP1 for a variety of input and output conditions, see Fig. 5. The input beam was varied from 5 to 20 mm in steps of 2.5 mm and from 10 to 50 mrad in steps of 10 mrad, with both transverse phase planes being identical ; the I/E values were changed from 3 to 6, in steps of 1, by varying E and keeping I fixed at 300 mA.

A very interesting result was found : for a given input beam size and divergence, the computed settings for T1 and T2 were essentially the same for all values of I/E . This fact can be understood by

a) the beam transport is space charge dominated, and according to formula (3.4) the required focusing is the same if $I/\beta E = I/\hat{x}^2$ does not change;

b) the conditions imposed at AP1 are such that for $I = \text{const}$, β and γ vary approximately as E^{-1} , thus keeping \hat{x} and \hat{x}' roughly the same ; compare Fig. 4.

Applying now the reasoning under a) and b) for different beam intensities, one finds that the same focusing will hold provided the input values for \hat{x} and \hat{x}' vary as $\sqrt{I/300}$. This fact has also been confirmed numerically.

A consequence of the above consideration is the general validity of the triplet settings of Fig. 5 : they do not depend on E and are applicable for all beam intensities provided the scales on the coordinate axis are $\sqrt{300/I} \hat{x}$ and $\sqrt{300/I} \hat{x}'$ respectively. On Fig. 6, the quadrupole strengths are replaced by the corresponding quadrupole currents.

All aperture limitations were ignored when searching for the triplet values of Fig. 5 ; they have been introduced in Fig. 7, where they delimit, together with the no-solution region, the LEBT acceptance.

The vacuum chamber aperture d along the LEBT is not constant, see Fig. 3. It is assumed that the beam hits the aperture limit when

$$2\hat{x} = 2\sqrt{6} \sqrt{x^2} \geq d ,$$

where $\sqrt{x^2}$ is the r.m.s. beam radius and \hat{x} the marginal one ; the factor $\sqrt{6}$ applies for a parabolic density distribution ¹⁾. In TRACE one works with a uniform density beam ("equivalent beam") having

$$\hat{x}_e = 2\sqrt{x^2} ;$$

hence all the apertures d have to be scaled as

$$\frac{d}{d_e} = \frac{\sqrt{6}}{2} \rightarrow d_e \cong 0.82 d .$$

Aperture limitations occur at :

- middle of T1 ($d_e/2 = 26.7$ mm)
- exit of T1 ($d_e/2 = 22.6$ mm)
- input of T2 ($d_e/2 = 27.5$ mm)
- middle of T2 ($d_e/2 = 37$ mm)

Taking, as example, the usual beams in LEBT one gets :

$$\left. \begin{aligned} I &= 200 \text{ mA} \\ E &= 50 \text{ mm mrad} \\ \beta &= 3\text{m} (\hat{x} \cong 12.5 \text{ mm}) \end{aligned} \right\} \sigma = 12$$

As $\sigma \gg 1$, the focusing in LEBT is strongly space charge dominated and formula (3.2) becomes :

$$K \cong K_0 \sigma \cong \frac{1}{\beta} \left[\text{m}^{-1} \right] \frac{I[\text{mA}]}{E[\text{mm mrad}]} . \quad (3.4)$$

The focusing depends on the ratio I/E (in what follows this ratio will always be quoted in above units) and inversely on β . Beams with different I/E can be transported with the same focusing, provided β is changed accordingly (I/\hat{x}^2 is to be kept constant).

In Fig. 4 are shown the conditions one imposes on the beam at AP1 ; they are a function of the ratio I/E only (see also ¹⁾). With these conditions and using TRACE, one has explored the range of input beams which can be accepted by LEBT.

At first one has calculated a set of quadrupole strengths for triplets T1 and T2 that produced a match at AP1 for a variety of input and output conditions, see Fig. 5. The input beam was varied from 5 to 20 mm in steps of 2.5 mm and from 10 to 50 mrad in steps of 10 mrad, with both transverse phase planes being identical ; the I/E values were changed from 3 to 6, in steps of 1, by varying E and keeping I fixed at 300 mA.

A very interesting result was found : for a given input beam size and divergence, the computed settings for T1 and T2 were essentially the same for all values of I/E . This fact can be understood by

a) the beam transport is space charge dominated, and according to formula (3.4) the required focusing is the same if $I/\beta E = I/\hat{x}^2$ does not change;

b) the conditions imposed at AP1 are such that for $I = \text{const}$, β and γ vary approximately as E^{-1} , thus keeping \hat{x} and \hat{x}' roughly the same ; compare Fig. 4.

Applying now the reasoning under a) and b) for different beam intensities, one finds that the same focusing will hold provided the input values for \hat{x} and \hat{x}' vary as $\sqrt{I/300}$. This fact has also been confirmed numerically.

A consequence of the above consideration is the general validity of the triplet settings of Fig. 5 : they do not depend on E and are applicable for all beam intensities provided the scales on the coordinate axis are $\sqrt{300/I} \hat{x}$ and $\sqrt{300/I} \hat{x}'$ respectively. On Fig. 6, the quadrupole strengths are replaced by the corresponding quadrupole currents.

All aperture limitations were ignored when searching for the triplet values of Fig. 5 ; they have been introduced in Fig. 7, where they delimit, together with the no-solution region, the LEBT acceptance.

The vacuum chamber aperture d along the LEBT is not constant, see Fig. 3. It is assumed that the beam hits the aperture limit when

$$2\hat{x} = 2\sqrt{6} \sqrt{x^2} \geq d ,$$

where $\sqrt{x^2}$ is the r.m.s. beam radius and \hat{x} the marginal one ; the factor $\sqrt{6}$ applies for a parabolic density distribution ¹⁾. In TRACE one works with a uniform density beam ("equivalent beam") having

$$\hat{x}_e = 2\sqrt{x^2} ;$$

hence all the apertures d have to be scaled as

$$\frac{d}{d_e} = \frac{\sqrt{6}}{2} \rightarrow d_e \cong 0.82 d .$$

Aperture limitations occur at :

- middle of T1 ($d_e/2 = 26.7$ mm)
- exit of T1 ($d_e/2 = 22.6$ mm)
- input of T2 ($d_e/2 = 27.5$ mm)
- middle of T2 ($d_e/2 = 37$ mm)

The limit at the middle of T2 is approached for a 300 mA beam over the entire range of acceptable input values. The limit at entrance to T2 is exceeded for all input conditions at currents above 350 mA. Beams having small radii and large divergences have the critical aperture at the exit of T1. The middle of T1 limits the acceptance on the right hand side of Fig. 7. The limits shown on this figure are for beam currents of 300 mA and 200 mA, to indicate how the acceptance region increases as the current is decreased.

For the sake of completeness, triplet settings in the second half of the unbunched beam section have also been calculated. The input conditions, at AP2, depend on I/E ; the output conditions, at mid-way between bunchers B1 and B2, are the same for all beams: $\hat{x} = \hat{y} = 5\text{mm}$, $\alpha = 0$. The results are presented in Fig. 8 (settings of T3 and T4), while Fig. 9 shows the envelope of a typical beam.

The Table of Fig. 8, which gives the settings of T3 and T4 for a variety of input values of I and I/E , contains more information than that. The beam dynamics depend only on $I/\beta E$ (see Eq. (3.4)); therefore, if one wants a smaller beam at the buncher, T3 and T4 values given for higher currents (but same I/E) could be used. For example, suppose $I = 200$ and $I/E = 5$. Then $T3 = (3.85/-3.67)$ and $T4 = (-3.54/3.42)$ would produce a 5mm waist at the buncher. Choosing T3 and T4 values corresponding to $I = 300$ and $I/E = 5$ would produce a waist at the buncher with radius $\sqrt{200/300} \cdot 5\text{mm}$. Choosing T3 and T4 values corresponding to $I = 100$ and $I/E = 5$ would produce a waist with radius $\sqrt{200/100} \cdot 5\text{mm}$. These facts have been confirmed by computation, compare Fig. 10 to Fig. 9.

The above analysis of acceptance and of triplet settings in the whole unbunched beam section of LEBT should contribute to have an understandable beam transport up to the buncher.

4. POSSIBILITIES OF REMOVING LEBT ACCEPTANCE LIMITATIONS

The LEBT has been designed by assuming a certain, reasonable range of input beam characteristics. Although these characteristics are even now not known with precision (some measuring equipment is still missing and ion source tests are going on), it seems that the LEBT acceptance is sufficient in order to meet the design specifications of the new linac.

However, it is certainly interesting to analyse briefly if and how some acceptance limitations mentioned in the previous chapter could eventually be removed.

- The aperture limitation at mid T1 is hard to remove, but it does not seem it will become critical ; limitations at exit of T1 and input of T2 can be removed by increasing the vacuum chamber diameter, which is presently smaller at these places, see Fig. 3.
- The no-solution region can be reduced by moving T2 closer to T1 (in which case, the steering coil ST2 and the sector valve SV1 would be installed after T2, see Fig. 3). In Fig. 11 one has indicated how the no-solution region is decreased by approaching T2 to T1 by 250 mm.
- The beam size at mid T2 is almost entirely determined by the distance T2-AP1 and by the conditions imposed at AP1. The beam size can be reduced by
 - a) moving AP1 closer to T2
 - b) reducing the distance AP1-AP2.

By moving AP1 50 mm closer to T2, the beam radius at mid T2 is reduced by approximately 2mm. A similar reduction is obtained by decreasing the spacing between AP1 and AP2 from 675mm to 550 mm, thereby changing the conditions required at AP1. Fig. 12b shows the result of doing both ; the same beam was before "just" contained in the aperture, see Fig. 12a. However, higher quadrupole gradients are needed in T1 and T2 to meet the new requirements.

Some of the measures for the reduction of acceptance limitations outlined above, ask for moving pieces of equipment up to 250 mm upstream. As the length of LEBT cannot be changed, this extra space has to be placed somewhere. In Fig. 13, three possibilities have been analysed :

- 1) increasing the distance between T4 and DDHB by 250 mm ;
- 2) increasing the distances between T3 and T4 and between T4 and DDHB by 100 and 150 mm, respectively ;
- 3) increasing the distance between T3 and T4 by 250 mm.

The best solution, as can be seen, in the last one, yielding smallest beam envelopes but with slightly increased quadrupole gradients. In all cases, the beam intensity was kept at 300 mA with $I/E = 5$.

At the end, the transport of high intensity beams was computed through the unbunched beam part of the actual LEBT, by ignoring conditions for beam intensity limitations at AP1. Fig. 14 shows how the same 300 mA beam as before can be matched to the buncher, by having now envelopes well within aperture limits everywhere (input beam conditions : $\hat{x} = 10$ mm, $\hat{x}' = 30$ mrad ; small input beams have usually large envelopes at mid T2). The same focusing setting permits also the transport of a 400 mA beam, again with $I/E = 5$, but with envelopes and divergences increased $\propto \sqrt{400/300}$, see Fig. 15.

5. PROCEDURE FOR THE ADJUSTMENT OF FOCUSING PARAMETERS

The focusing parameters of LEBT are adjusted by a procedure based on a combined use of beam measuring facilities and of the transport program TRACE. According to Fig. 3, there are four triplets (unbunched beam section) and six quadrupoles (bunching section) to be set. At the present state of LEBT the parameter settings are more difficult to be controlled, since several measuring devices are not installed yet, see Fig. 3.

The only emittance measuring apparatus now in use is EM2 ; therefore the present adjustment procedure is the following :

- a) measure emittance at EM2 and intensity at IM2 and IM3 ;
- b) transfer measured emittance to LEBT input by TRACE ;
- c) adjust triplets T1 and T2 in order to fulfill conditions at AP1 (done by the optimizing routine of TRACE) ;
- d) remeasure emittance at EM2 with new settings of T1 and T2 ;
- e) transfer emittance to input of T3 by TRACE ;
- f) adjust triplets T3 and T4 in order to meet conditions at the buncher DDHB (use optimizing routine of TRACE) ;
- g) transfer beam by TRACE from DDHB to Linac input ; use optimising routine to adjust quadrupoles and meet Linac input conditions (only four out of six quadrupoles can be adjusted at a time, hence the optimisation has to be done in a few steps).

The points a) to f) serve to bring the beam correctly to the buncher ;

the most important condition there is the beam size (in future checked by the beam profile measuring device PM). The step g) matches the beam to the linac input (in future checked by the emittance device EM3).

As example, an adjustment procedure is outlined in Figs. 16 to 25. The following comments apply :

- Fig. 16 : measured beam emittances ;
- Fig. 17 : the result of the beam transfer to LEBT input is somewhat unrealistic, as the input beam is not rotationally symmetric (what is in reality the case). This discrepancy is due to accumulated errors in a rather long beam transfer and will in future be avoided by the installation of EM1. As far as transfer errors are concerned, there are reasons to believe that the conversion of quadrupole currents into focusing strengths is not absolutely correct; how important this is can be seen from Fig. 18, where the beam transfer to LEBT input is done by changing the focusing strength of the outer quadrupoles of T2 and T3 by a mere 2.5%. The input beam is now roughly rotationally symmetric.

For the programme TRACE it can be said in general that it gives good precision for relative adjustments ; the precision of absolute settings drops with the length of transfer.

- Figs 19 to 22 are self explanatory.
- Figs 23 to 25 treat the matching in the bunching section, with no bunchers, one (B1) and two bunchers (B1 et B2) working, respectively. The third buncher (B3) has not yet been in operation.

The focusing adjustment procedure described so far has been adopted during the 10 MeV low intensity beam tests (accelerated beams \sim 50 mA) ; readjustments of quadrupole gradients, undertaken during the tests, have not brought any increase in the accelerated current. More tests are necessary in order to assess the real validity of the procedure.

It should be noted that TRACE treats a bunched beam in an approximative way : it is supposed that the bunch shrinks linearly between the buncher DDHB and the Linac (justified assumption, compare ¹⁾) ; the transverse space charge force at position "s" after the buncher is then obtained by multiplying the unbunched beam force by a factor ⁵⁾

$$\frac{1}{1 - \frac{1}{D} \left(1 - \frac{\Delta\phi^0}{180\eta} \right)},$$

where D distance buncher-linac
 $\Delta\phi$ half bunch extension at Linac
 η trapping efficiency

The emittance increase in the bunchers (except B3) is calculated according to Refs. 5), 6); B3 is treated as a linear defocusing lens.

6. OPERATION OF LEBT - Final state

The weak point of the adjustment procedure outlined in the previous chapter is the lack of test possibilities. This situation will be improved with the installation of still missing measuring devices. The planned adjustment procedure will then be :

- a) measure beam emittance at EM1 and intensity at IM2 ;
- b) transfer to LEBT input by TRACE ;
- c) match to AP1 by TRACE (adjustment of T1 and T2) ;
- d) check matching at AP1 by a temporary installed emittance device EM2' ; this device will be removed after assessing a confidence degree to the matching. Measure intensity at IM3.
- d) match from AP1 to midway between B1 and B2 by TRACE ; check matching at EM2 and PM and intensity at IM4 and IM5 ; introduce focusing corrections if necessary ;
- e) match from DDHB to linac input by TRACE ; check matching at EM3 and intensity at IM6 ; use also 10 MeV measuring facilities (beam transformer and profile device).

Note that the emittance device EM3 measures the emittance of the total beam, whilst one is interested in the emittance of trapped particles only. Corrections to be applied can be calculated accordingly ⁶⁾, but are not discussed in this paper.

The matching parameters at Linac input are computed by the program LINEF ⁷⁾.

7. CONCLUSION

It was felt necessary to specify the beam transfer possibilities of LEBT in a comprehensive way. The knowledge of its acceptance and limitations is important for the present operation and eventual future plans.

The review of adjustment procedures shows how focusing parameters can be set in a controllable manner ; approximate beam envelopes in the whole LEBT can be displayed on the screen using TRACE. Even if focusing readjustments might become necessary, they can be carried out in an understandable way by using measuring and computing devices.

The quality of LEBT adjustments will undergo the best test during the systematic 10 MeV beam measurements (autumn 1977) ; some evolution in the adjustment procedures could be expected.

R E F E R E N C E S

- 1) B. Bru and M. Weiss, "Design of the low energy beam transport system for the new 50 MeV linac", CERN/MPS/LIN 74-1.
- 2) K. Crandall "TRACE, an interactive on-line beam transport program for unbunched beams", PS/LIN/Note 77-3.
- 3) B. Montague "private communication".
- 4) D.J. Warner and M. Weiss "Beam optics in the CERN new 50 MeV linac", CERN/PS/LIN 76-2, and 1976 Proton Linear Acc. Conf., Chalk River, Canada.
- 5) K. Crandall, "Addendum to program TRACE", CERN/PS/LIN Note 77-15.
- 6) M. Weiss "Bunching of intense proton beams with six-dimensional matching to the Linac acceptance", CERN/MPS/LIN 73-2 and 1973 Particle Acc. Conf., San Francisco, USA.
- 7) B. Bru, J. Guyard and M. Weiss "Optimization programs dealing with beam optics in the complex of the linear accelerator", in preparation.

A P P E N D I X

MAXIMUM FOCUSING STRENGTH OF A SYMMETRIC TRIPLET

It will be shown that a simple relation exists between the maximum focusing strength (equal in both planes) and the length of a symmetric triplet.

Following an analysis done by B. Montague³⁾, a symmetric triplet composed of three thin quadrupoles will be considered ; see Fig. 1a. Thin quadrupoles make the analysis clearer, without losing its generality ; the results are applicable to thick quadrupoles with minor, unessential corrections.

The transfer matrix of the triplet of Fig. 1a is

$$M = \begin{pmatrix} m_{11} & m_{12} \\ \Delta & m_{22} \end{pmatrix} = \begin{bmatrix} 1 + \ell(\delta_i + 2\delta_0) + \ell\delta_i\delta_0 & \ell(2 + \ell\delta_i) \\ (\delta_i + 2\delta_0 + \ell\delta_i\delta_0)(1 + \ell\delta_0) & \ell\delta_0(2 + \ell\delta_i) + \ell\delta_i + 1 \end{bmatrix}.$$

For a focusing or defocusing quadrupole, δ_i and δ_0 are negative or positive respectively. The focusing term of the triplet is Δ ; multiplying it by ℓ and putting $\delta_0\ell = u$ and $\delta_i\ell = v$ one gets a dimensionless factor Q :

$$Q = (v + 2u + uv)(1 + u) = v(1 + u)^2 + 2u(1 + u). \quad (1)$$

If, e.g., the above expression holds for the x plane, in the y plane one has :

$$Q_y = -v(1 - u)^2 - 2u(1 - u), \quad (2)$$

Q_x and Q_y are functions of u and v . The condition for equal focusing in both planes gives :

$$Q_x = Q_y \rightarrow v = -\frac{2u}{1 + u^2}. \quad (3)$$

The Q 's are now functions of one variable only :

$$Q_x(u) = -\frac{2u}{1+u^2} (1+u)^2 + 2u(1+u) . \quad (4)$$

Extremum : $dQ_x/du = 0$, which gives when arranged

$$u^5 + 2u^3 - u = 0 ;$$

the interesting solutions are :

$$u_{1,2} = \pm \sqrt{\sqrt{2} - 1} \cong \pm 0.6436 \quad (5)$$

The corresponding v :

$$v_{1,2} = \mp \sqrt{2(\sqrt{2} - 1)} \cong \mp 0.91 (= \mp \sqrt{2} u) . \quad (6)$$

From the last expression one sees that a thin quadrupole triplet has its maximum strength when the inner quadrupole is $\sqrt{2}$ times stronger than the outer. For the maximum strength one gets :

$$Q_x \max = Q_y \max = \Delta_{\max} \cdot \ell = 4\sqrt{2} - 6 \cong -0.342$$

or

$$\Delta_{\max} = \frac{Q_{\max}}{\ell} = -\frac{0.342}{\ell} . \quad (7)$$

The last result is very interesting : the shorter the triplet, the stronger Δ_{\max} which can in principle be obtained, see Fig. 1b.

For completeness sake, the position of principal planes of the triplet (counted from triplet centre) is also given :

$$p = \ell \frac{u}{1+u} ; \quad (8)$$

it is interesting that p depends only on the strength of the outer quadrupole.

The above analysis remains in principle valid also for thick quadrupole triplets, the difference being that Q_{\max} is slightly reduced ; this fact, however, does not take off the generality of the conclusions.

A P P E N D I X

PERMISSIBLE DISTANCE BETWEEN TRIPLETS

A system consisting of two thin triplets separated by a distance L is presented in Fig. 2a ; the transfer matrix of this system is

$$T = \begin{pmatrix} t_{11} & t_{12} \\ t_{21} & t_{22} \end{pmatrix} = \begin{pmatrix} 1 + L\Delta_1 & L \\ \Delta_1 + \Delta_2 + L\Delta_1\Delta_2 & 1 + L\Delta_2 \end{pmatrix} .$$

Neglecting the space charge, a beam is transported through this system by the formula :

$$S_n = TST^T = \begin{pmatrix} t_{11} & t_{12} \\ t_{21} & t_{22} \end{pmatrix} \begin{pmatrix} \beta & -\alpha \\ -\alpha & \gamma \end{pmatrix} \begin{pmatrix} t_{11} & t_{21} \\ t_{12} & t_{22} \end{pmatrix} = \begin{pmatrix} t_{11}^2\beta - t_{11}t_{12}\cdot 2\alpha + t_{12}^2\gamma & t_{11}t_{21}\beta - (t_{11}t_{22} + t_{12}t_{21})\alpha + t_{12}t_{22}\gamma \\ t_{11}t_{21}\beta - (t_{11}t_{22} + t_{12}t_{21})\alpha + t_{12}t_{22}\gamma & t_{21}^2\beta - t_{21}t_{22}\cdot 2\alpha + t_{22}^2\gamma \end{pmatrix} \quad (1)$$

where S is the inverse of the matrix of the quadratic form, specifying the input beam ellipse :

$$\gamma x^2 + 2\alpha xx' + \beta x'^2 = E .$$

The parameters of the output ellipse β_n , α_n and γ_n , calculated by the formula (1) are :

$$\beta_n = t_{11}^2\beta - 2t_{11}t_{12}\alpha + t_{12}^2\gamma \quad (2)$$

$$\alpha_n = (t_{11}t_{22} + t_{12}t_{21})\alpha - t_{11}t_{21}\beta - t_{12}t_{22}\gamma \quad (3)$$

$$\gamma_n = t_{21}^2\beta - 2t_{11}t_{12}\alpha + t_{22}^2\gamma . \quad (4)$$

If one imposes β_n (i.e., the beam size), Eq. (2) can be solved for t_{11} (note that $t_{12} = L$) :

$$t_{11} = L \left(\frac{\alpha}{\beta} \pm \sqrt{\frac{\alpha^2}{\beta^2} - \frac{\gamma}{\beta} + \frac{1}{L^2} \frac{\beta_n}{\beta}} \right), \quad (5)$$

and introducing from the transfer matrix $t_{11} = 1 + L\Delta_1$ one obtains :

$$\Delta_1 = \frac{\alpha}{\beta} - \frac{1}{L} \pm \sqrt{-\frac{1}{\beta^2} + \frac{1}{L^2} \frac{\beta_n}{\beta}}. \quad (6)$$

Real solutions for Δ_1 exist if the discriminant > 0 ; this requirement is fulfilled with the condition :

$$L < \sqrt{\beta\beta_n}. \quad (7)$$

The same condition applies also for Δ_2 ; this is demonstrated in the simplest way by transporting the beam backwards through the system of Fig. 2a and getting for Δ_2 :

$$\Delta_2 = -\frac{\alpha_n}{\beta_n} - \frac{1}{L} \pm \sqrt{-\frac{1}{\beta_n^2} + \frac{1}{L^2} \frac{\beta}{\beta_n}};$$

the analysis of the discriminant leads to formula (7).

If one wishes to include space charge into consideration, one can do it in an approximate way by introducing an equivalent space charge lens Δ_{sc} into the transport system, see Fig. 2b. The transfer matrix of this system is :

$$T = \begin{pmatrix} t_{11} & t_{12} \\ t_{21} & t_{22} \end{pmatrix} = \begin{pmatrix} 1 & 0 \\ \Delta_2 & 1 \end{pmatrix} \begin{pmatrix} 1 & L/2 \\ 0 & 1 \end{pmatrix} \begin{pmatrix} 1 & 0 \\ \Delta_{sc} & 1 \end{pmatrix} \begin{pmatrix} 1 & L/2 \\ 0 & 1 \end{pmatrix} \begin{pmatrix} 1 & 0 \\ \Delta_1 & 1 \end{pmatrix} =$$

$$= \begin{bmatrix} 1 + L\Delta_1 + L/2 \Delta_{sc} + L^2/4 \Delta_1 \Delta_{sc} & L + L^2/4 \Delta_{sc} \\ \Delta_1 + \Delta_2 + \Delta_{sc} + L/2 \left(\Delta_1 \Delta_{sc} + \Delta_2 \Delta_{sc} + 2\Delta_1 \Delta_2 \right) + L^2/4 \Delta_1 \Delta_2 \Delta_{sc} & 1 + L\Delta_2 + L/2 \Delta_{sc} + L^2/4 \Delta_1 \Delta_{sc} \end{bmatrix}$$

Proceeding as before (see Eq. (4)), one obtains :

$$t_{11} = t_{12} \left(\frac{\alpha}{\beta} \pm \sqrt{-\frac{1}{\beta^2} + \frac{\beta_n}{\beta} \frac{1}{t_{12}^2}} \right)$$

and substituting t_{11} and t_{12} by their expressions

$$\Delta_1 = \frac{\alpha}{\beta} - \frac{1 + L/2 \Delta_{sc}}{L + L^2/4 \Delta_{sc}} \pm \sqrt{-\frac{1}{\beta^2} + \frac{\beta_n}{\beta} \frac{1}{(L + L^2/4 \Delta_{sc})^2}}$$

and analogously

$$\Delta_2 = -\frac{\alpha_n}{\beta_n} - \frac{1 + L/2 \Delta_{sc}}{L + L^2/4 \Delta_{sc}} \pm \sqrt{-\frac{1}{\beta_n^2} + \frac{\beta}{\beta_n} \frac{1}{(L + L^2/4 \Delta_{sc})^2}} .$$

The condition for matching solutions to exist is now :

$$L \left(1 + \frac{L \Delta_{sc}}{4} \right) \leq \sqrt{\beta \beta_n} \quad (8)$$

or

$$L = \frac{2}{\Delta_{sc}} \left(\sqrt{1 + \Delta_{sc} \sqrt{\beta \beta_n}} - 1 \right) . \quad (9)$$

Example :

In the unbunched beam part of LEBT, the beam intensity and radius are approximately :

$$\begin{aligned} I &= 300 \text{ mA} \\ \hat{r} &= 15 \text{ mm} . \end{aligned}$$

The distance between triplets : $L \approx 1.5 \text{ m}$

The space charge lens :

$$\Delta_{sc} = \frac{I \cdot e \cdot L}{2\pi \epsilon_0 m v^3 \hat{r}^2} \cong 2 \text{ m}^{-1} .$$

According to (8), the condition on β for the above case is :

$$\sqrt{\beta \beta_n} \geq 2.63 \text{ m} .$$

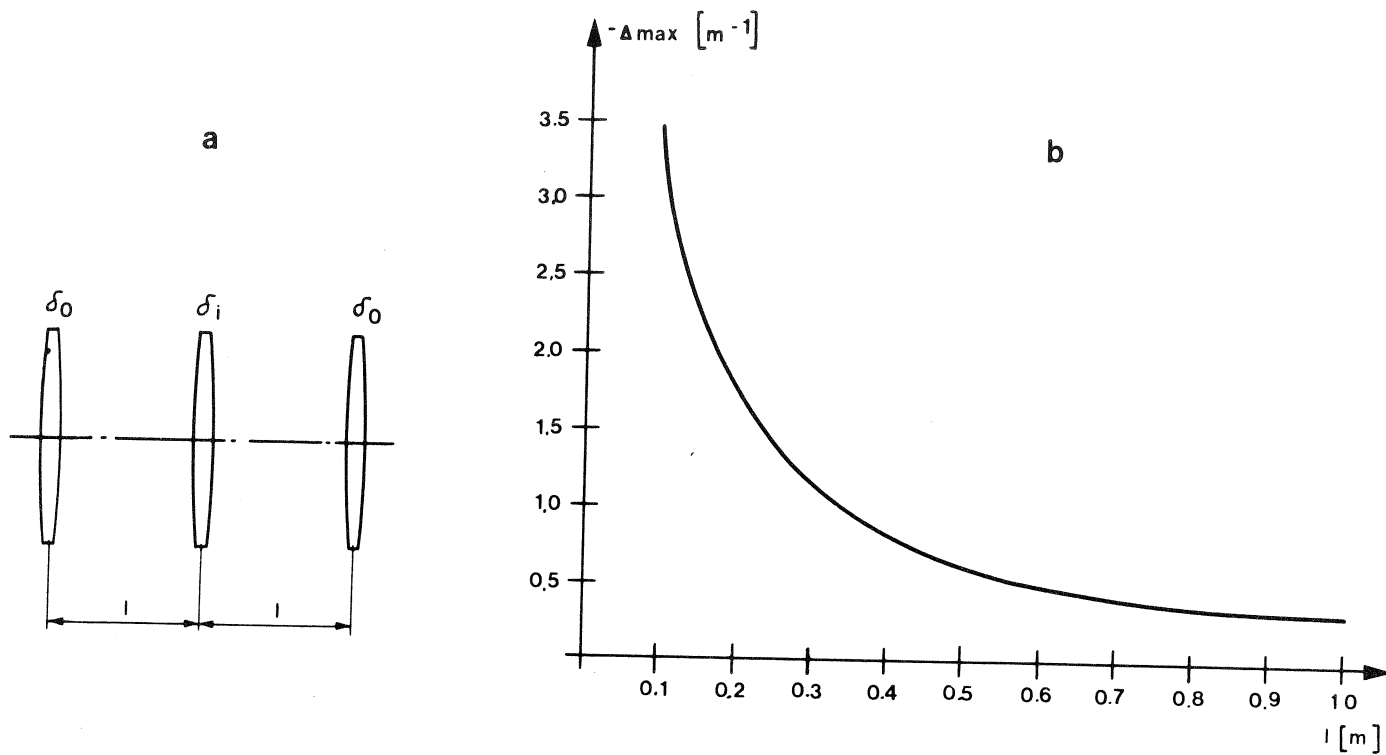


FIG. 1: Symmetric thin quadrupole triplet and its maximum focusing strength as function of l

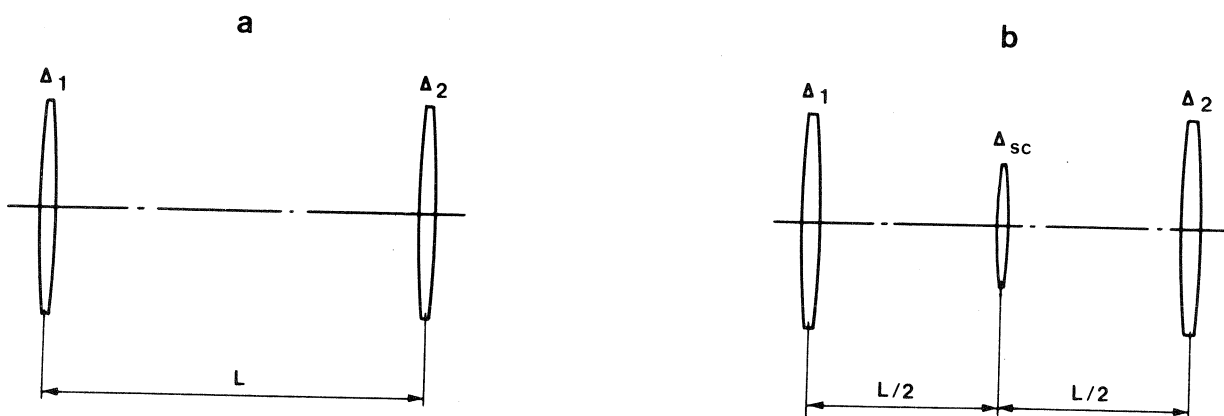


FIG. 2: System of two triplets Δ_1 and Δ_2 and the equivalent space charge lens Δ_{sc}

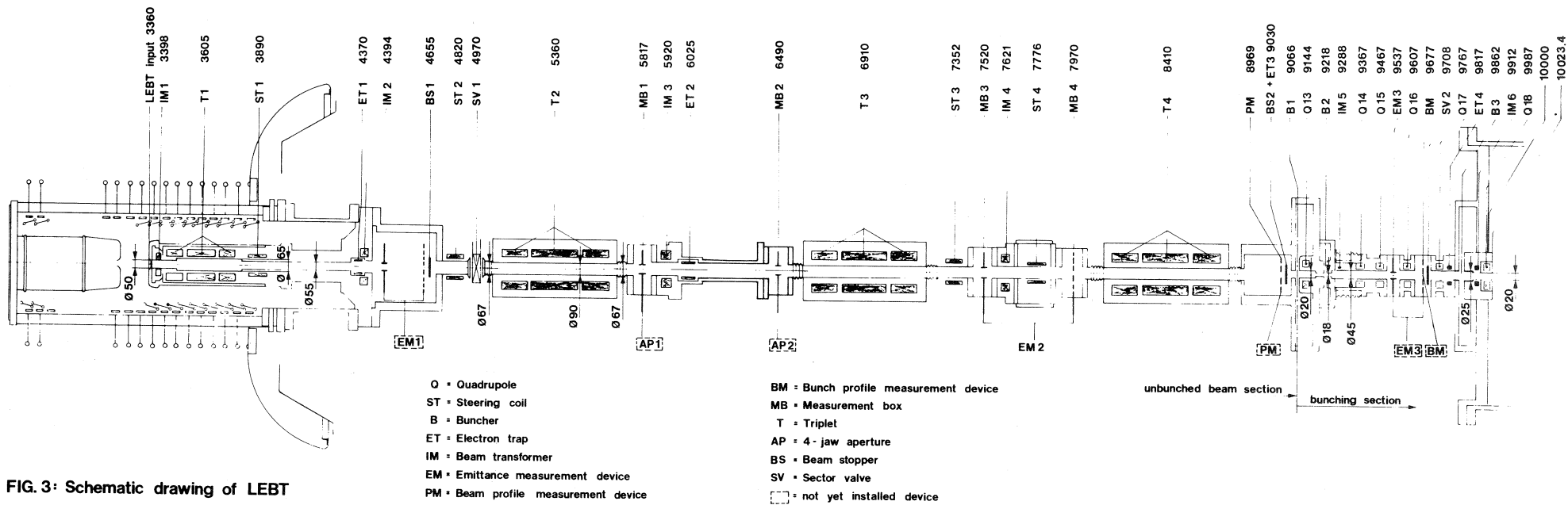
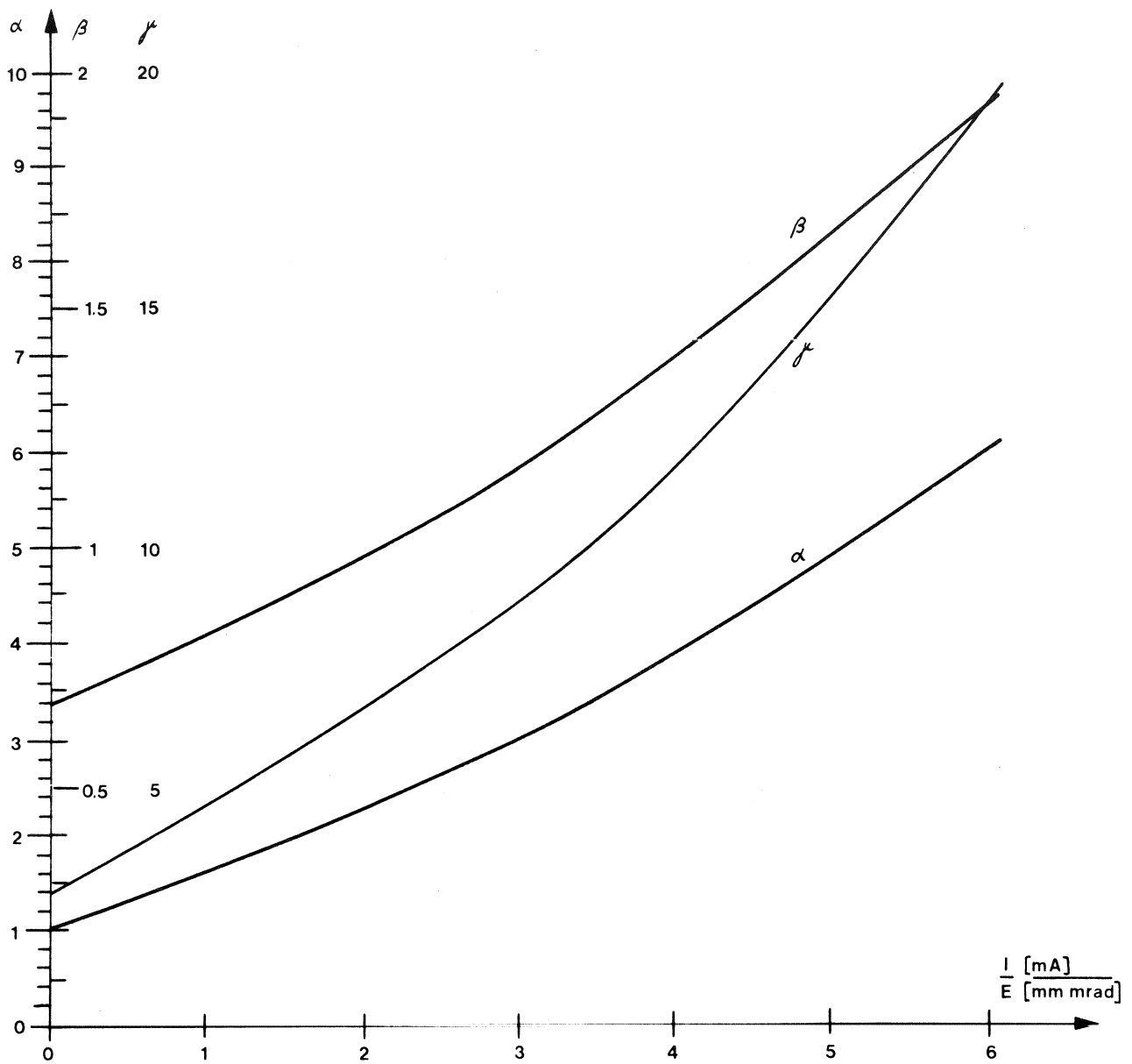


FIG. 3: Schematic drawing of LEBT



a) Conditions for nominal limiting section; $L_L = 675$ mm

b) Conditions for limiting sections of different L [mm]

$\frac{I}{E} \backslash L$	200	400	600	800	1000
1 α	1.510	2.100	2.763	3.502	4.332
1 β	0.236	0.559	0.984	1.533	2.221
2 α	1.695	2.529	3.504	4.614	5.859
2 β	0.249	0.621	1.147	1.859	2.790
3 α	1.895	3.000	4.350	5.889	7.633
3 β	0.263	0.689	1.333	2.239	3.457
4 α	2.098	3.508	5.235	7.259	9.567
4 β	0.277	0.763	1.530	2.650	4.191

FIG. 4: Conditions at AP1 for a proportional beam limitation

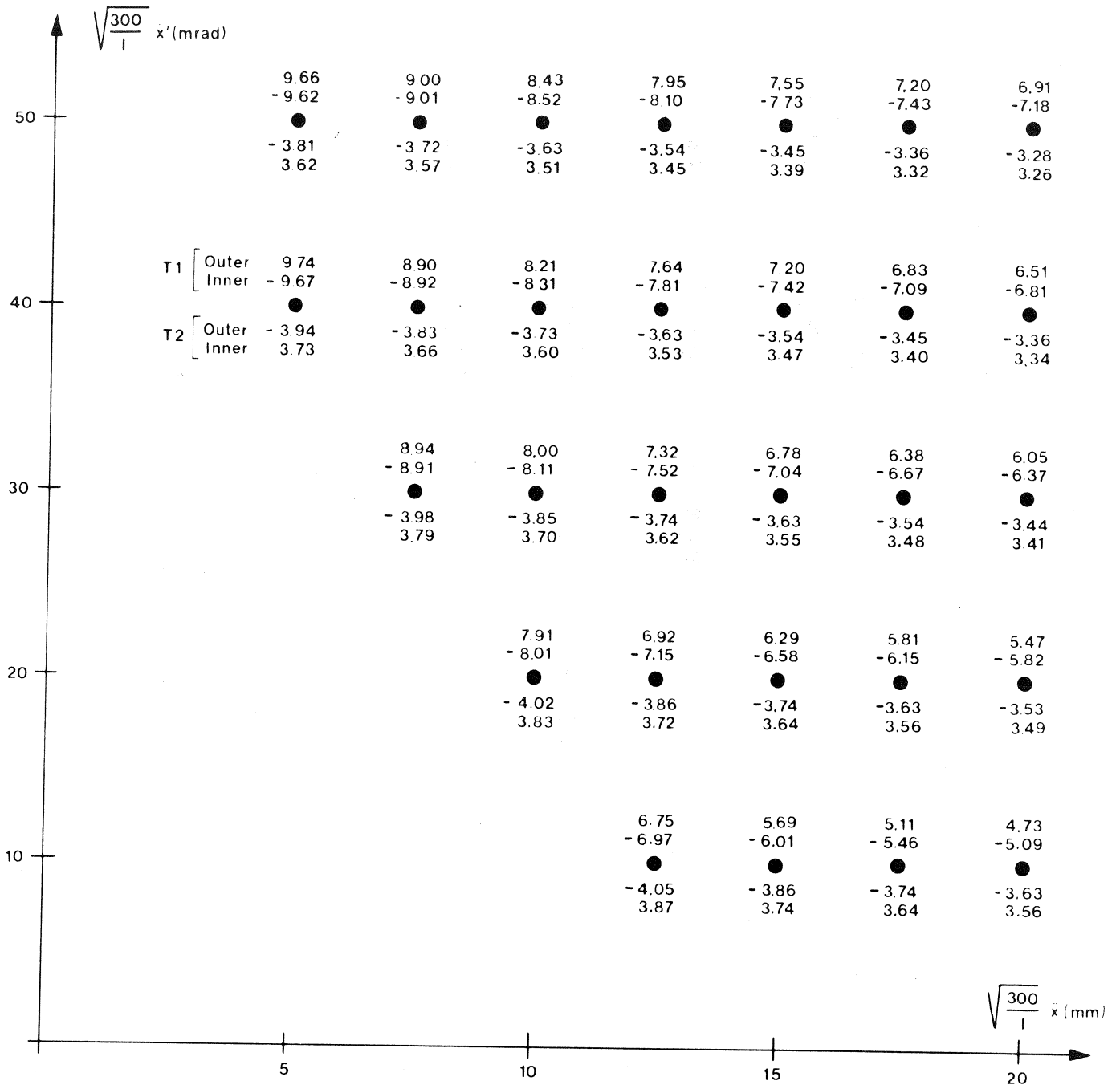


FIG. 5: Settings of triplets T1 and T2 for various input beams

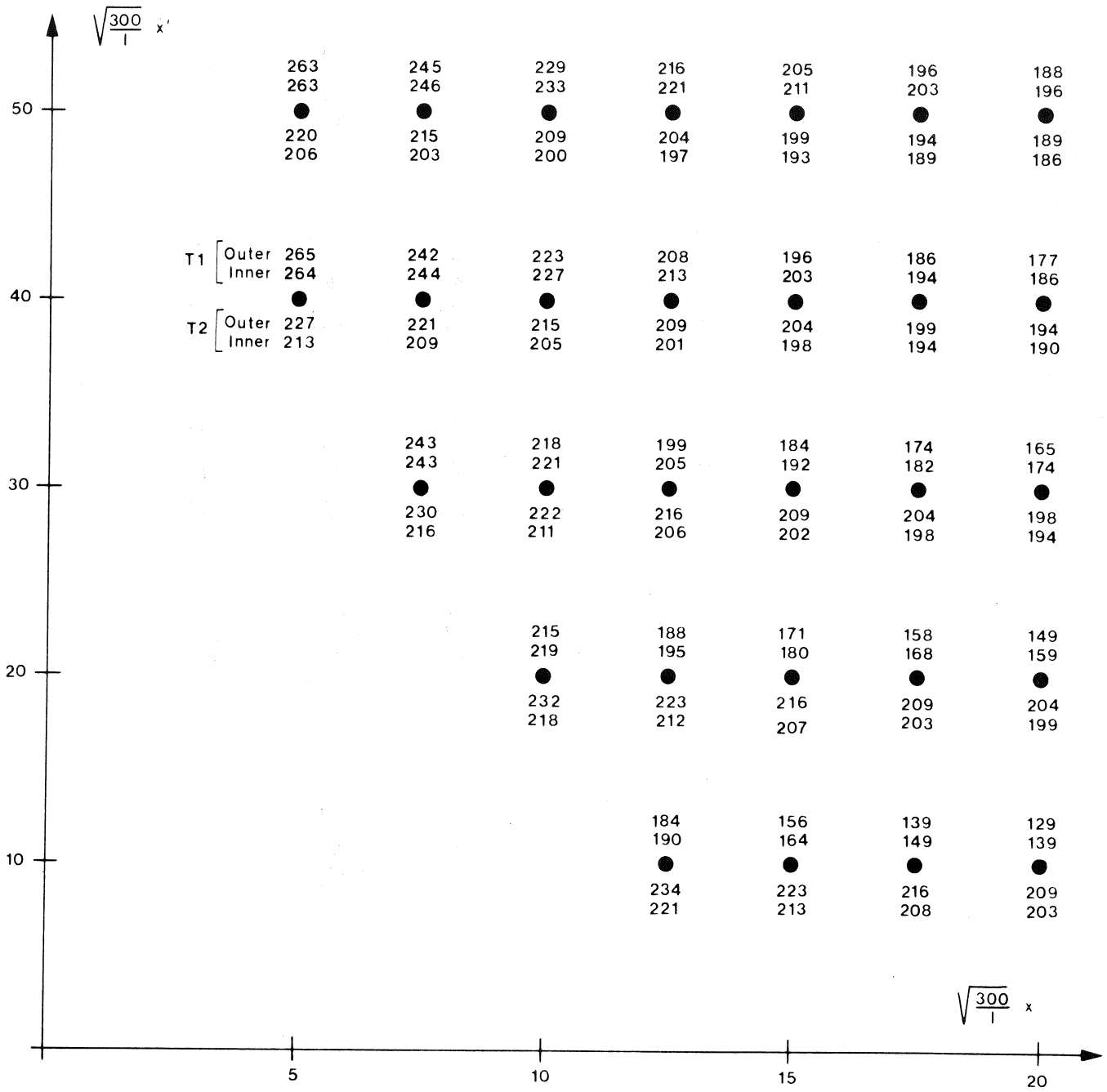


FIG.6: Currents of triplets T1 and T2 for various input beams

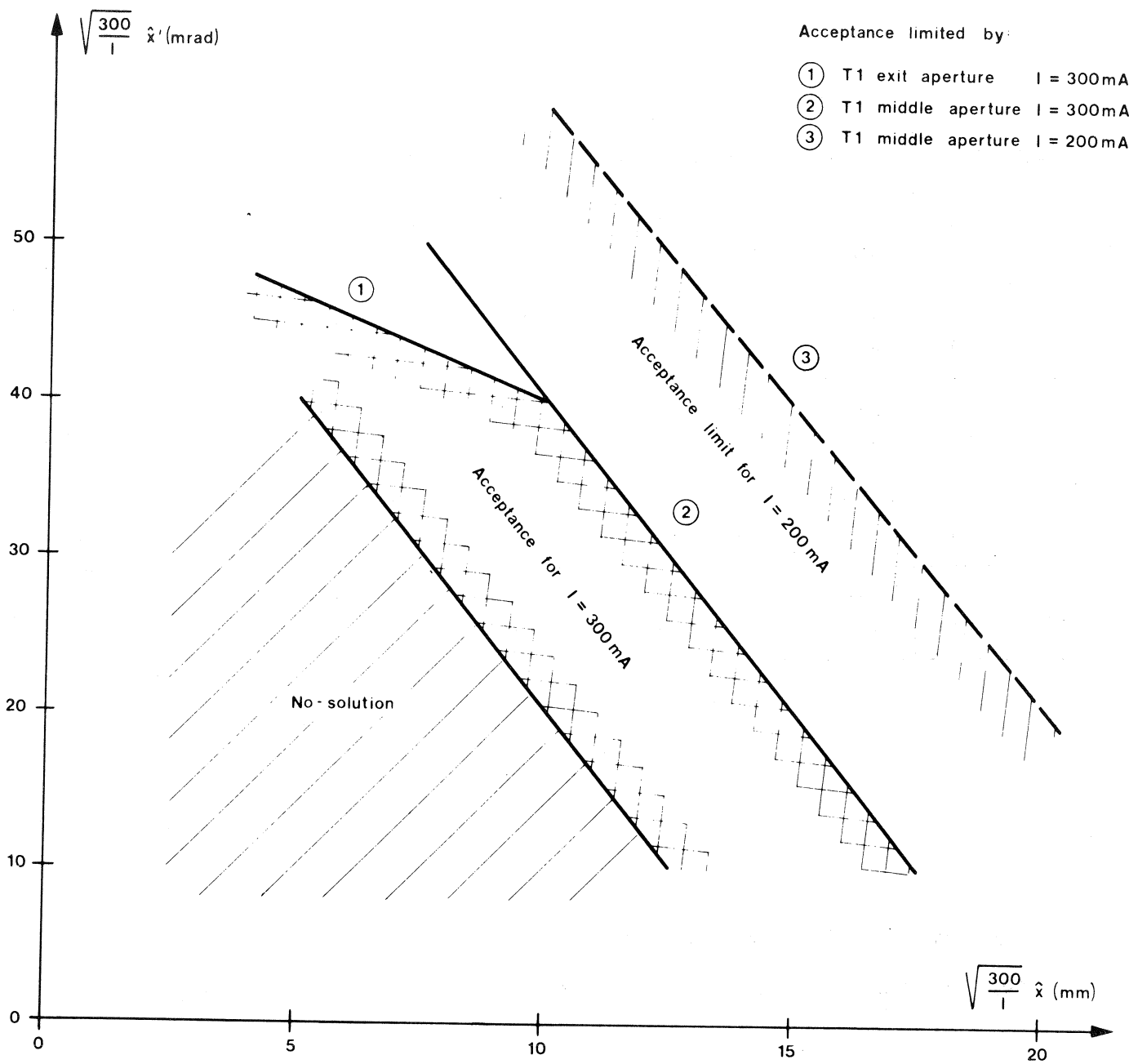


FIG. 7: Acceptance of LEBT with matching conditions at AP1

I [mA]	I/E	3		4		5		6	
		OUTER	INNER	OUTER	INNER	OUTER	INNER	OUTER	INNER
100	T3	3.77	-3.63	3.85	-3.69	3.89	-3.72	3.91	-3.74
	T4	-3.34	3.26	-3.31	3.23	-3.27	3.20	-3.23	3.16
150	T3	3.72	-3.57	3.82	-3.66	3.87	-3.70	3.90	-3.72
	T4	-3.47	3.36	-3.47	3.36	-3.45	3.34	-3.42	3.31
200	T3	3.66	-3.52	3.78	-3.62	3.85	-3.67	3.88	-3.70
	T4	-3.52	3.41	-3.54	3.42	-3.54	3.42	-3.51	3.39
250	T3	3.60	-3.47	3.74	-3.58	3.81	-3.64	3.85	-3.67
	T4	-3.55	3.43	-3.58	3.45	-3.58	3.45	-3.56	3.43
300	T3	3.55	-3.42	3.70	-3.54	3.78	-3.61	3.83	-3.65
	T4	-3.56	3.44	-3.59	3.46	-3.61	3.47	-3.59	3.46

FIG. 8: Settings for triplets T3 and T4 for various input conditions
Output condition: $\hat{x} = \hat{y} = 5 \text{ mm}$, $\alpha = 0$ at midway between B1 and B2

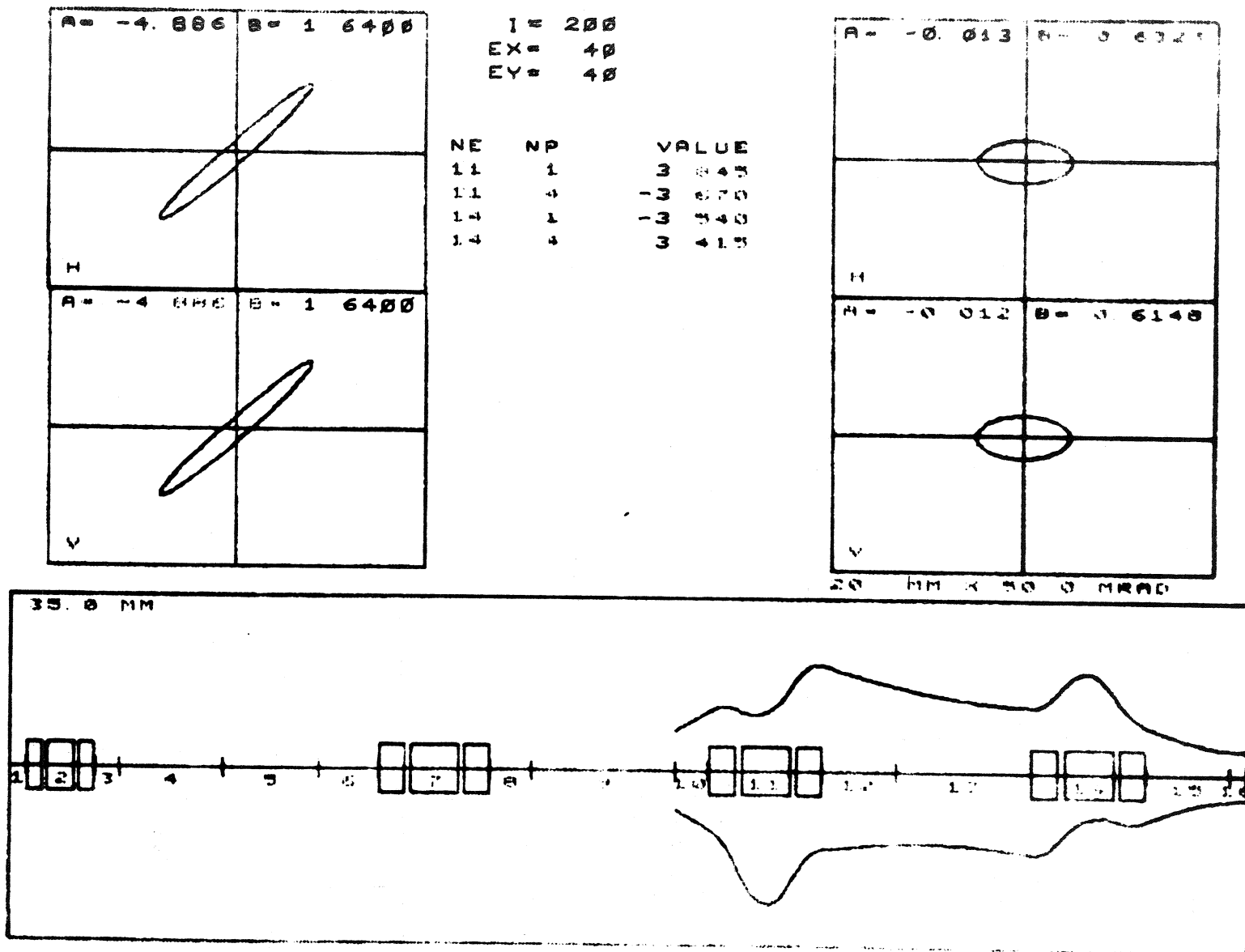
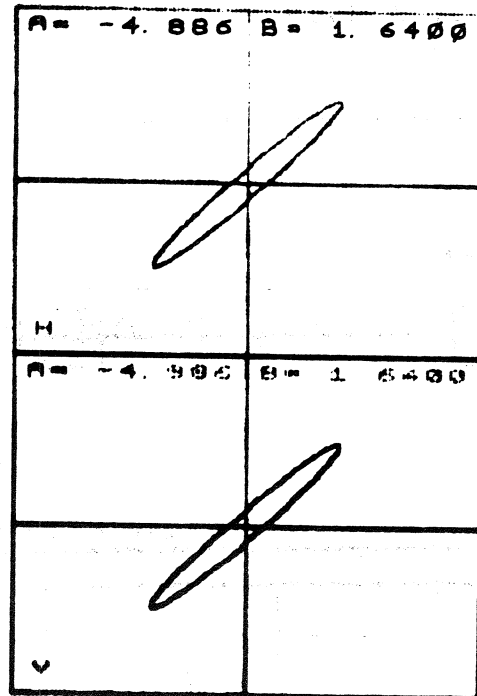


FIG. 9: Beam envelope in the 2nd half of the unbunched beam section; I = 200mA, I/E = 5



I = 200
EX = 40
EY = 40

NE	NP	VALUE
11	1	3.780
11	4	-3.611
14	1	-3.613
14	4	3.478

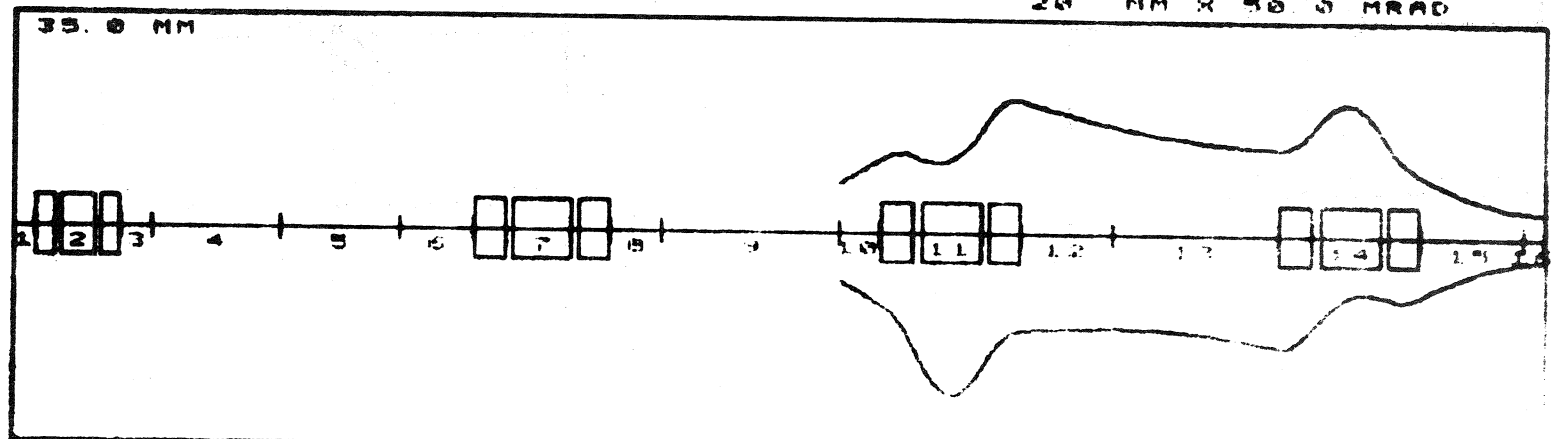
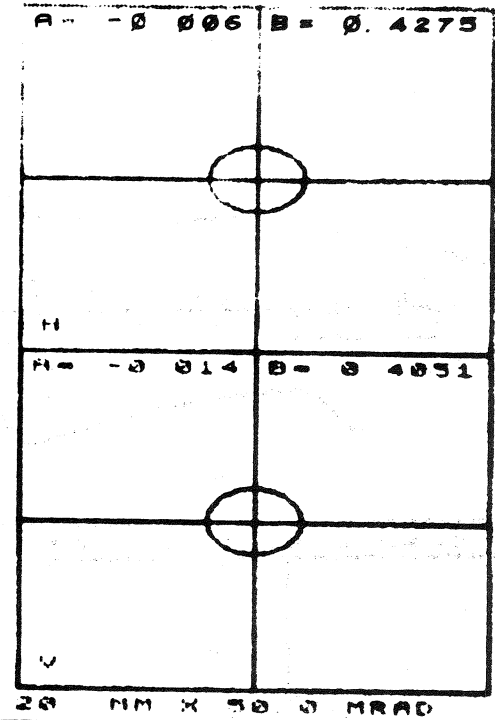


FIG.10: Same beam as on Fig. 9 but with a focusing corresponding to $I=300\text{mA}$ and $I/E=5$
(Note the reduced beam size at mid B1 - B2)

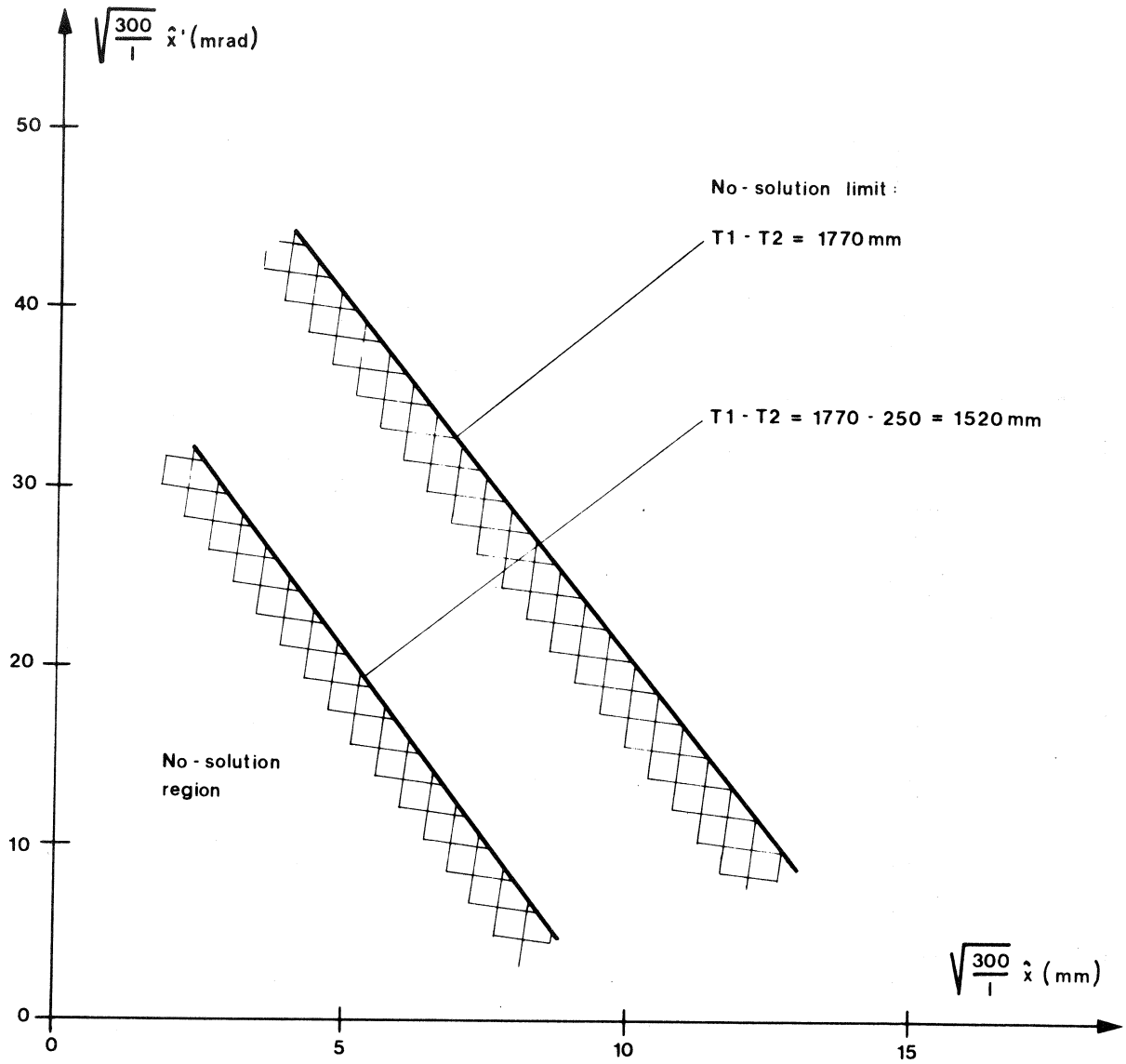
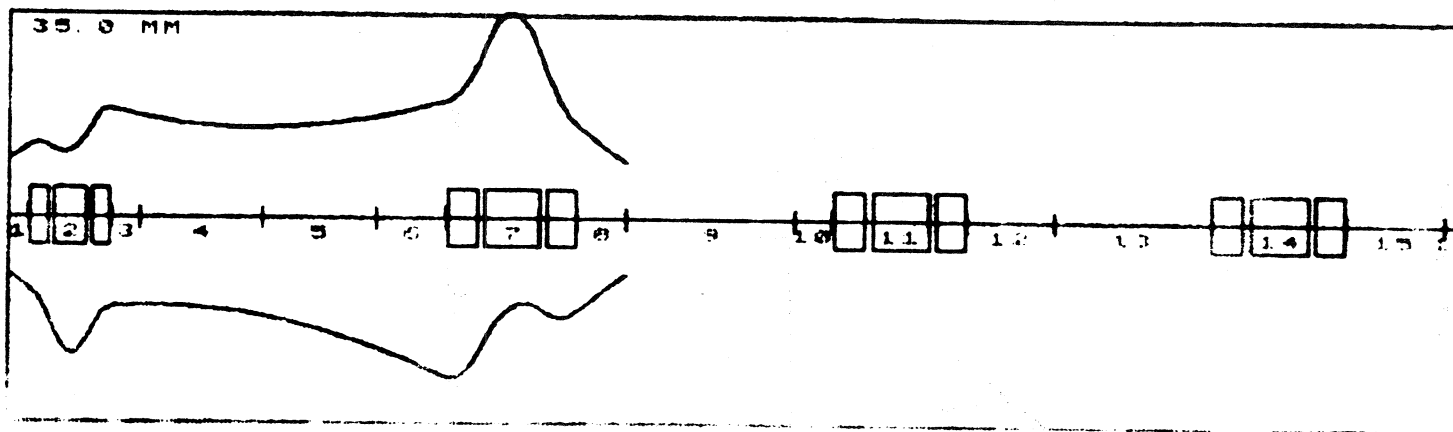


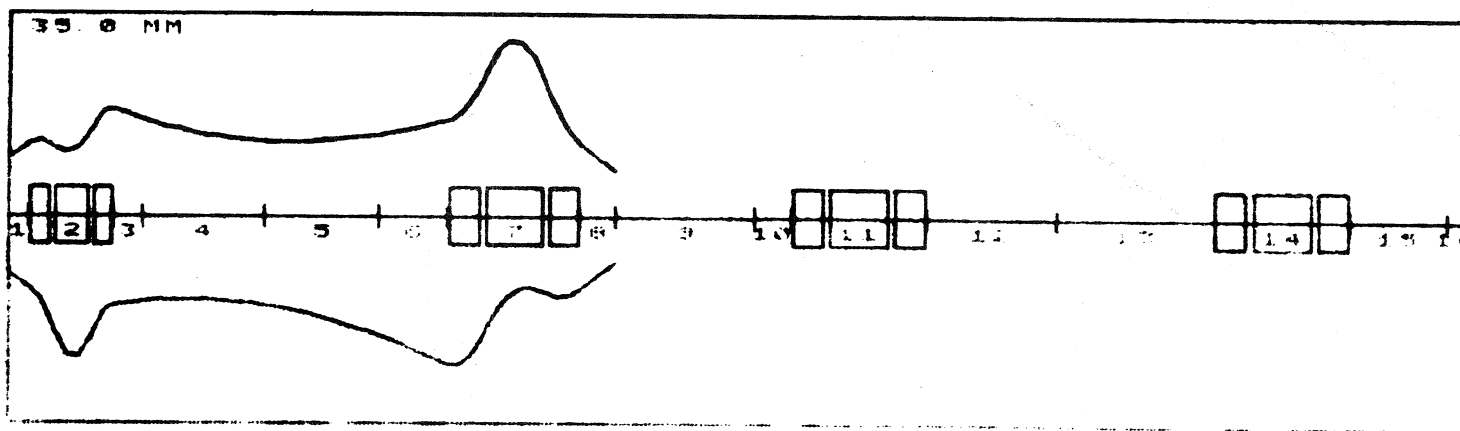
FIG. 11: Reduction of no-solution region by approaching T2 to T1 by 250 mm



I = 300
EX = 50
EY = 50

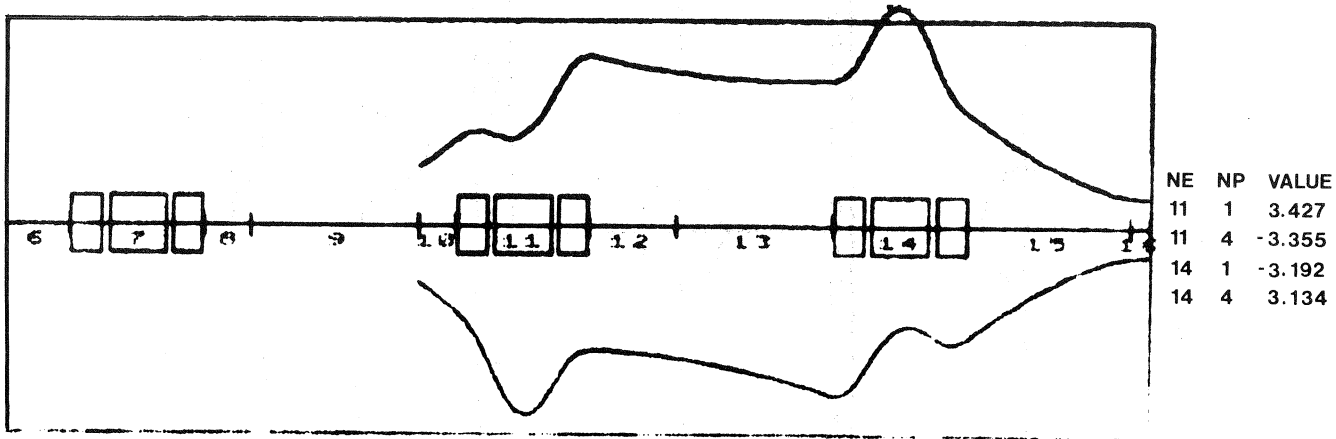
NE	NP	VALUE
2	1	8.000
2	4	-8.110
7	1	-3.850
7	4	3.700

FIG.12a: Beam envelope in the first part of LEBT

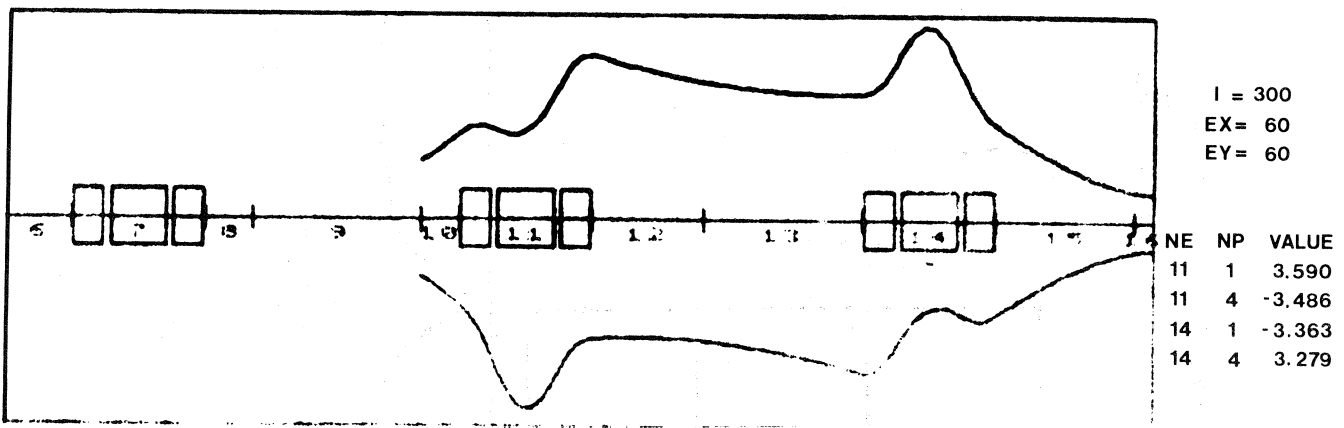


NE	NP	VALUE
2	1	8.407
2	4	-8.407
7	1	-4.197
7	4	3.974

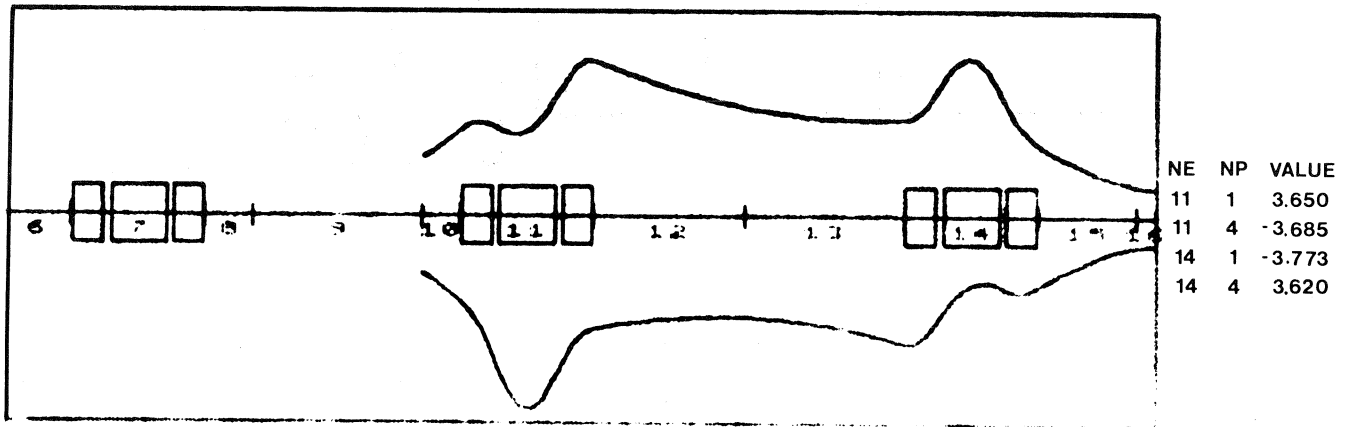
FIG.12b: Reduction of beam size at mid T2 by shortening AP1 - AP2 by 125mm and approaching AP1 to T2 by 50mm



a: Distance T4 - B1 increased by 250mm

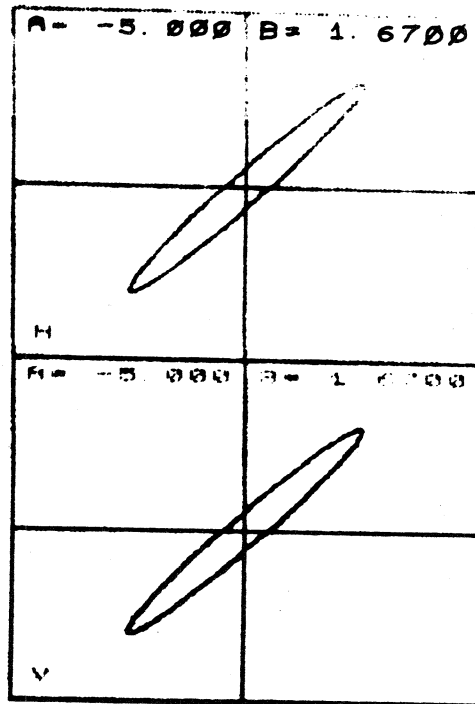


b: Distance T3 - T4 increased by 100mm
Distance T4 - B1 increased by 150mm



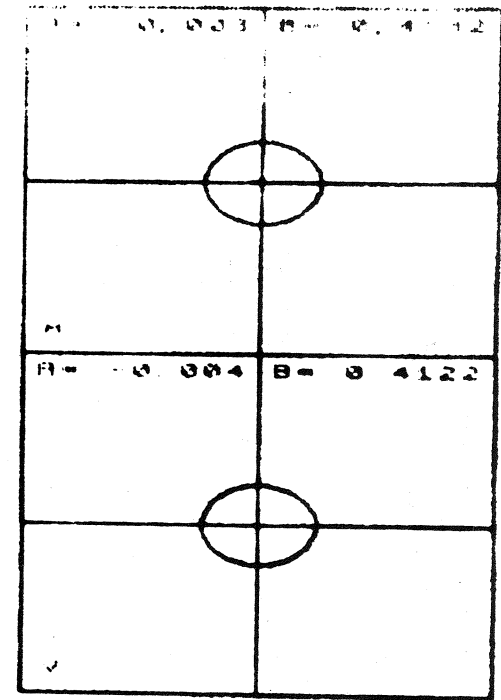
c: Distance T3 - T4 increased by 250mm

FIG. 13: Beam envelopes in the 2nd half of unbunched beam section



I = 300
EX = 60
EY = 60

NP	NP	VALUE
1	1	0.000
2	4	0.000
3	1	0.000
4	4	0.000
11	1	2.000
11	4	2.004
14	1	-0.000
14	4	0.000



20 MM X 50.0 MRAD

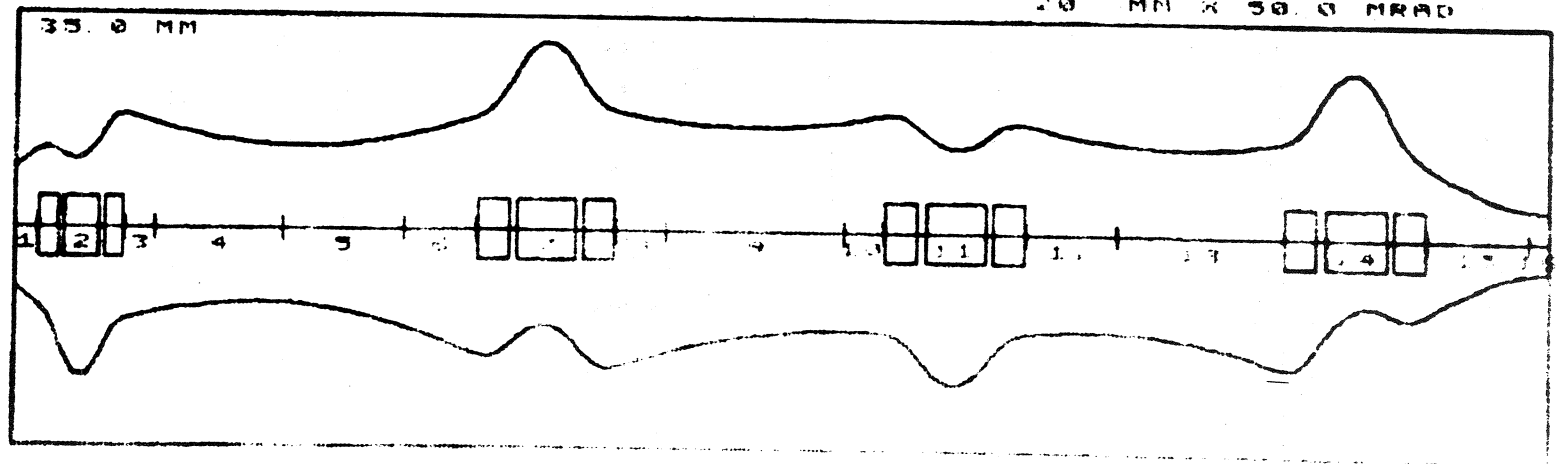


FIG.14: Transport of a 300mA beam, I/E = 5, with limiting conditions at AP1 ignored

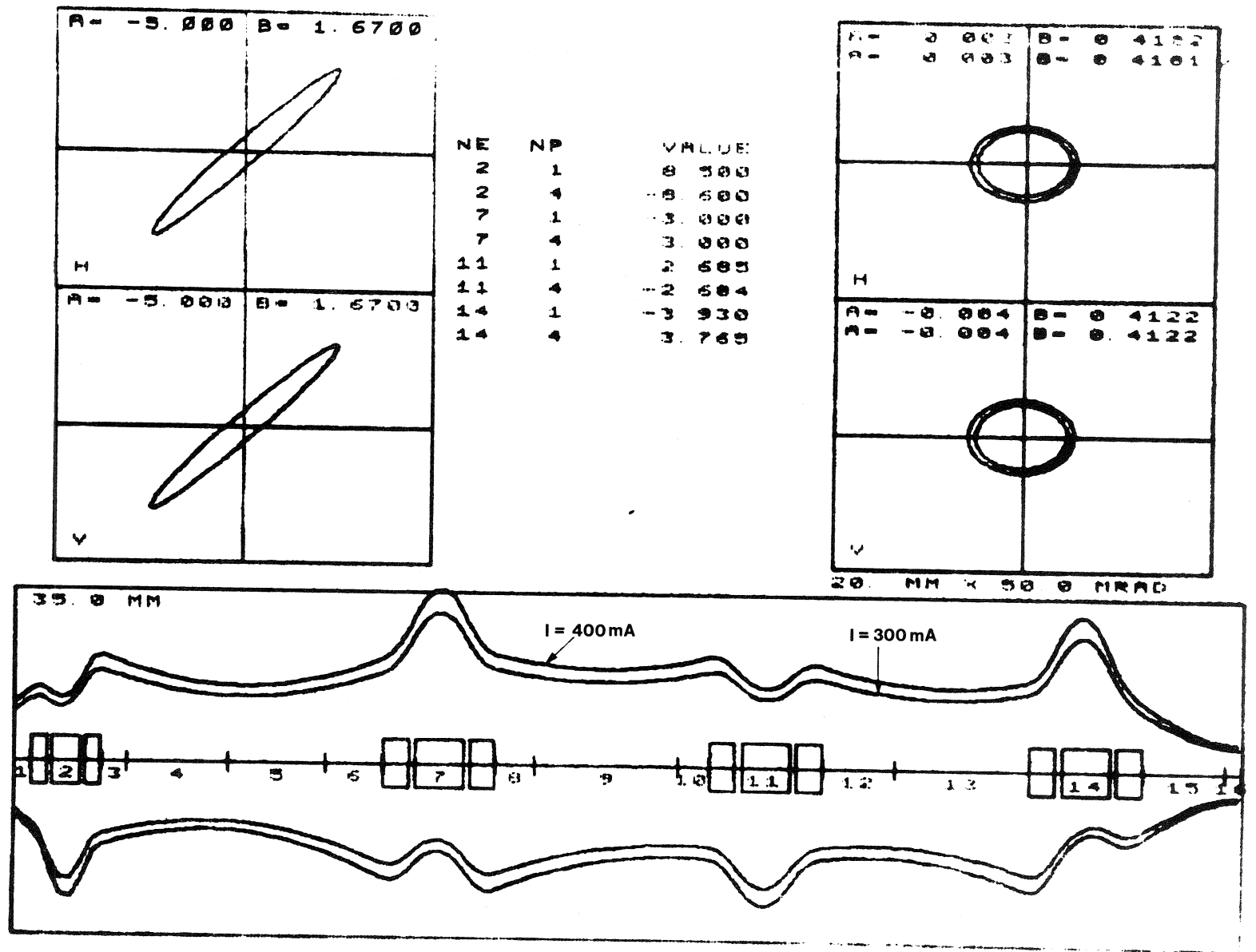
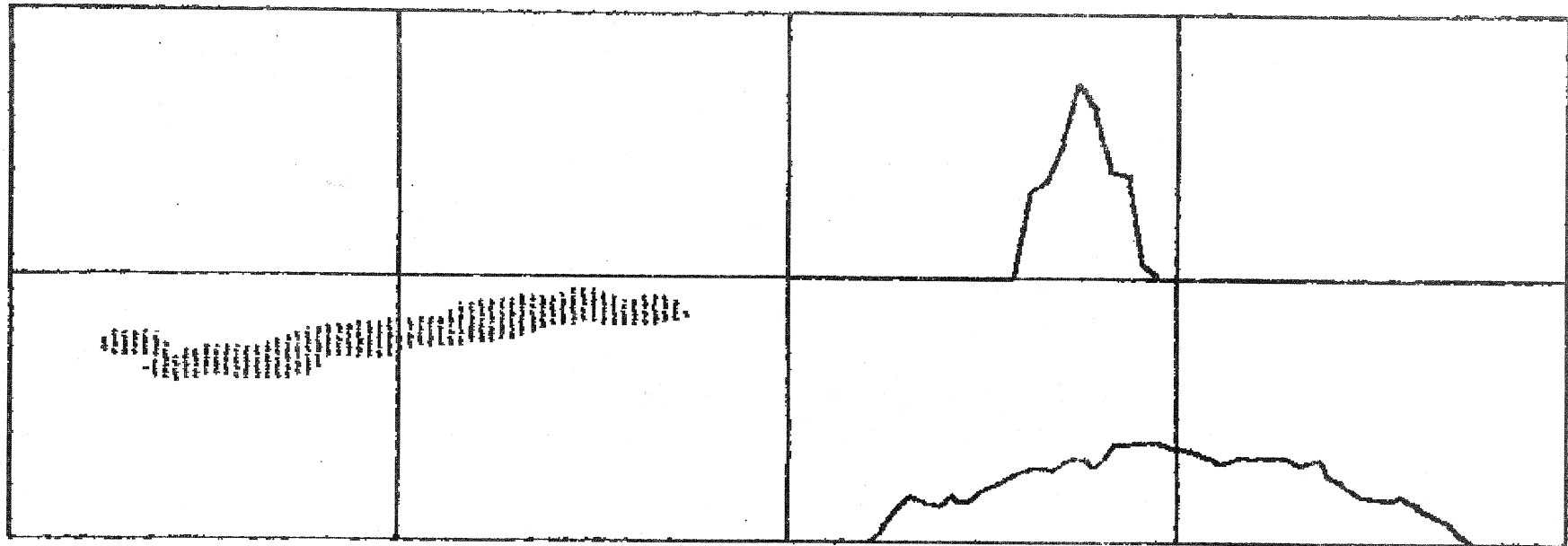


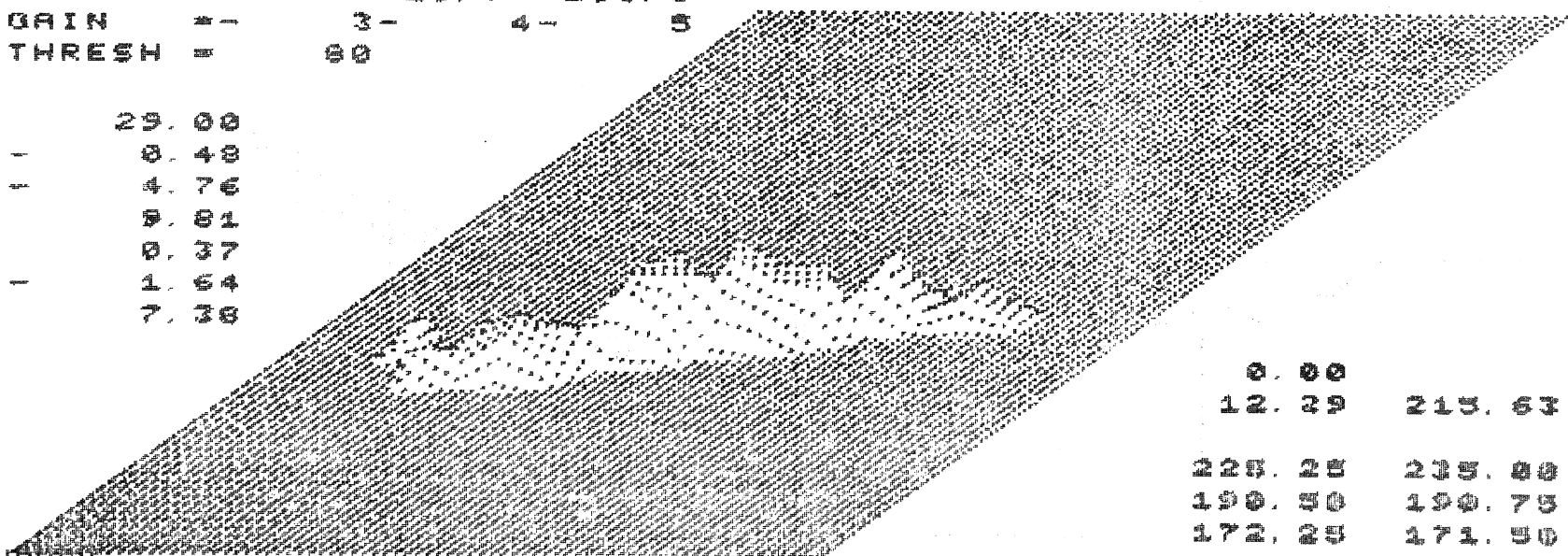
FIG.15: Transport of 300 and 400 mA beams, $I/E = 5$, with limiting conditions at AP1 ignored

750 KEY EMITTANCE MEASUREMENT - EM2 H - DATE: 77- 6-16



EM1300. W48. 1
 < 47. 5+ 41. 7> 23. 7 133. 8
 GAIN = - 3 - 4 - 8
 THRESH = 80

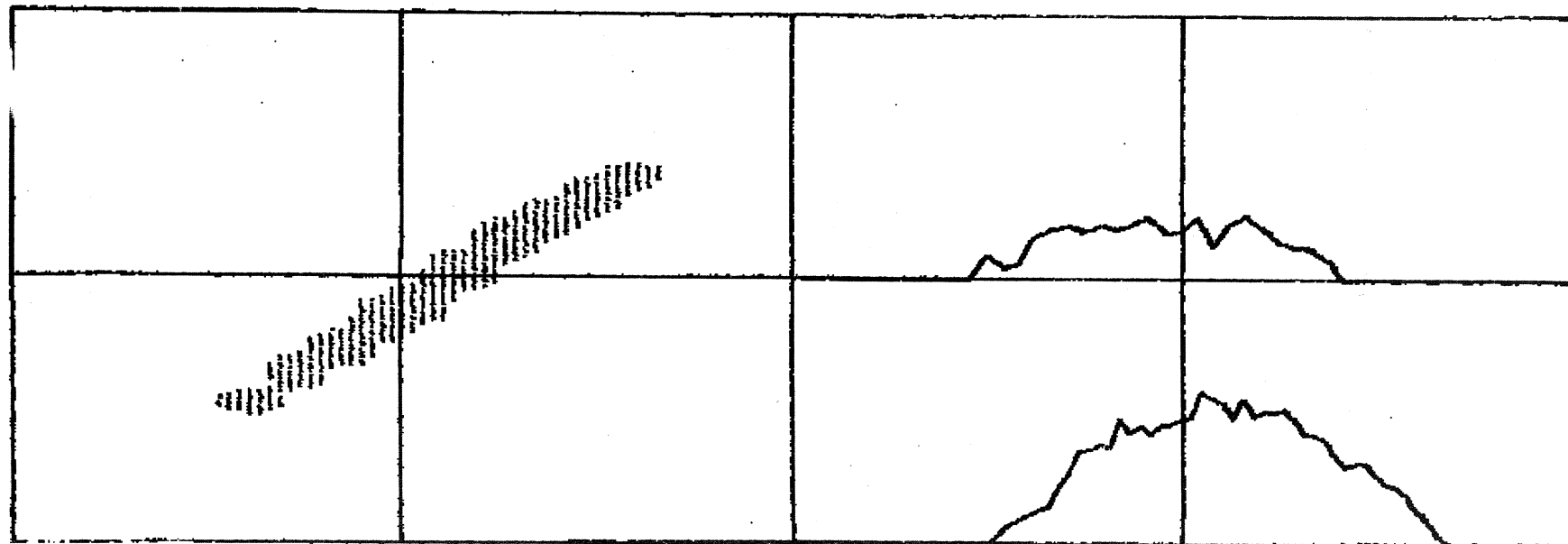
29. 00
 - 0. 40
 - 4. 76
 - 9. 01
 - 0. 37
 - 1. 64
 - 7. 40



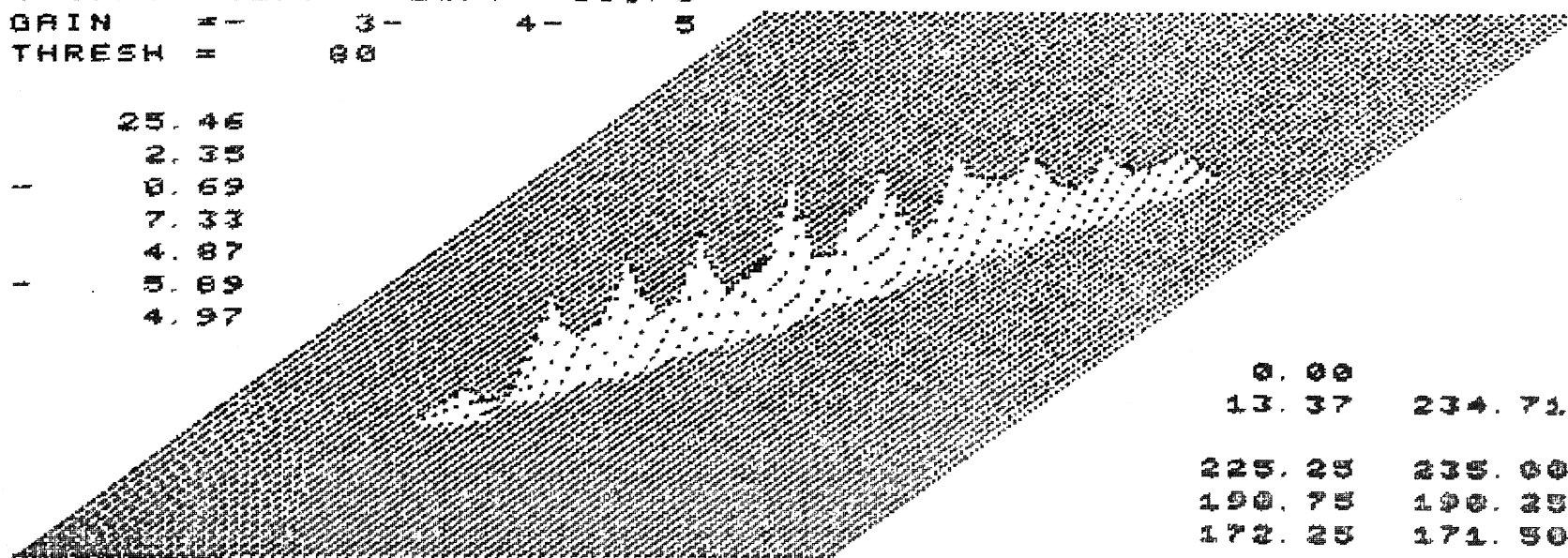
0. 00
 12. 29 215. 63
 228. 28 235. 86
 190. 50 190. 75
 172. 25 171. 50

FIG. 16a: Measured horizontal beam emittance at EM2

KEY EMITTANCE MEASUREMENT - EM2 V - DATE: 77- 6-16



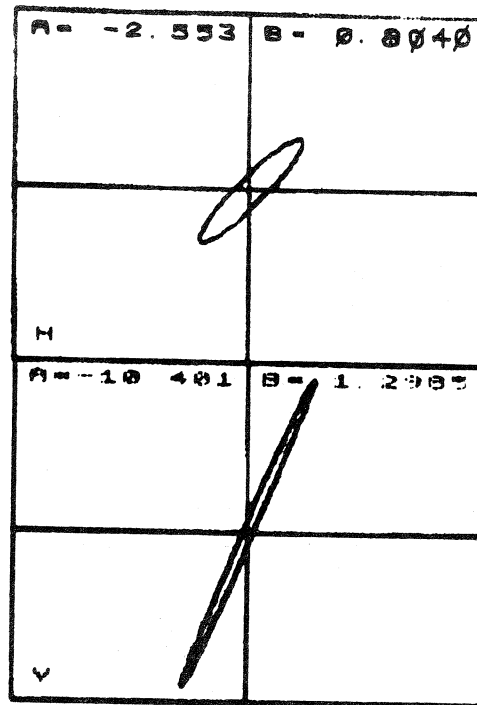
EM1389. W48; 1
 (47.5* 41.7) 23.7 133.8
 DRIN # - 3 - 4 - 5
 THRESH # 00



25.45
 2.35
 0.69
 7.44
 4.87
 3.89
 4.97

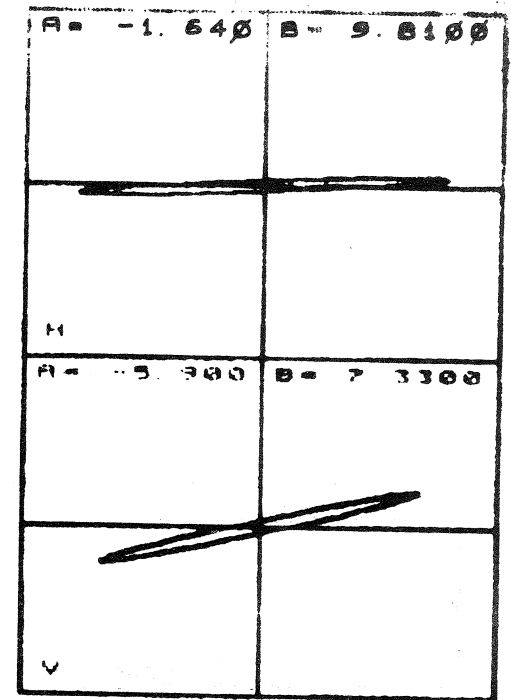
0.00
 13.37 234.71
 225.25 235.00
 190.75 190.25
 172.25 171.50

FIG. 16b: Measured vertical beam emittance at EM2



1 = 90
EX = 25
EY = 25

NE	NP	VALUE
2	1	225.000
2	4	230.000
7	1	190.000
7	4	191.000
11	1	172.000
11	4	171.000



20 MM X 50 0 MRAD

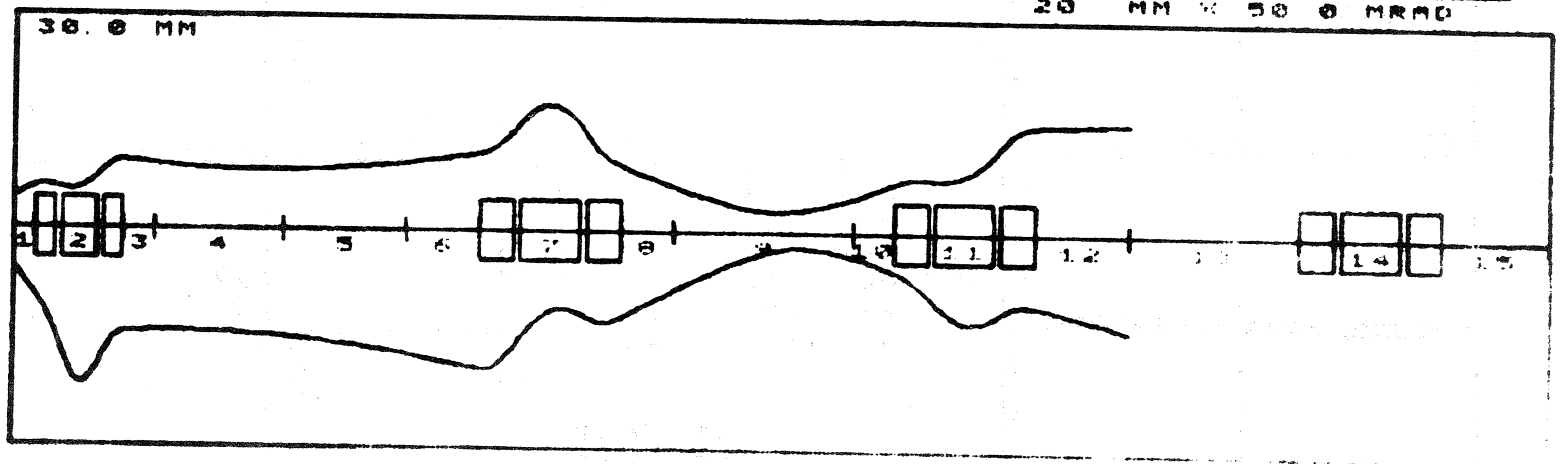
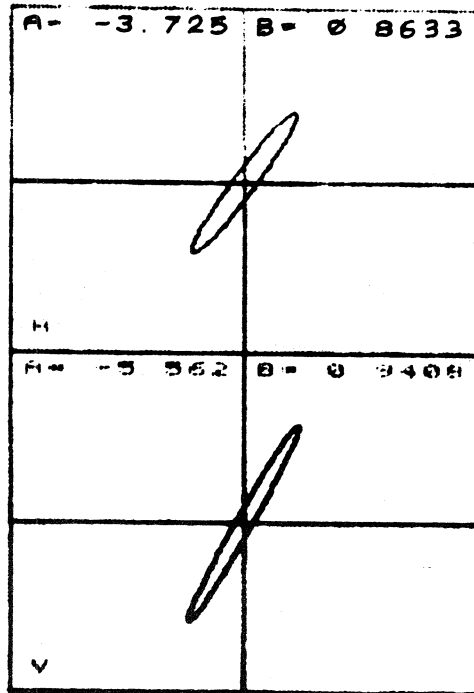


FIG. 17: Transfer of emittances measured at EM2 to LEBT input



I = 90
EX = 25
EY = 25

NE	NP	VALUE
2	1	225 000
2	4	-236 000
7	1	-195 000
7	4	191 000
11	1	176 000
11	4	-167 000

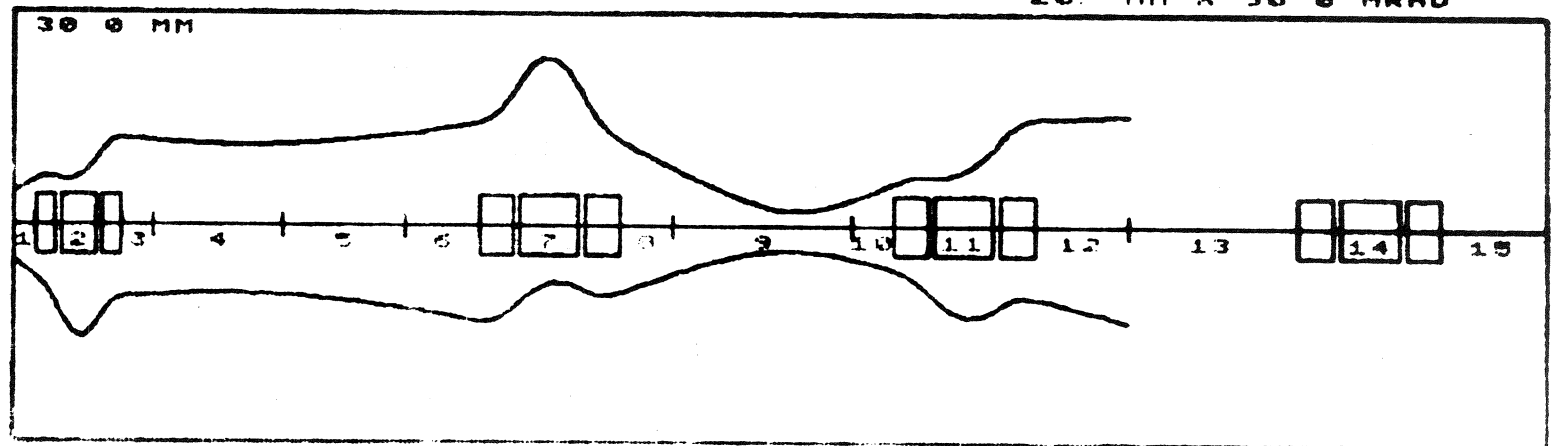
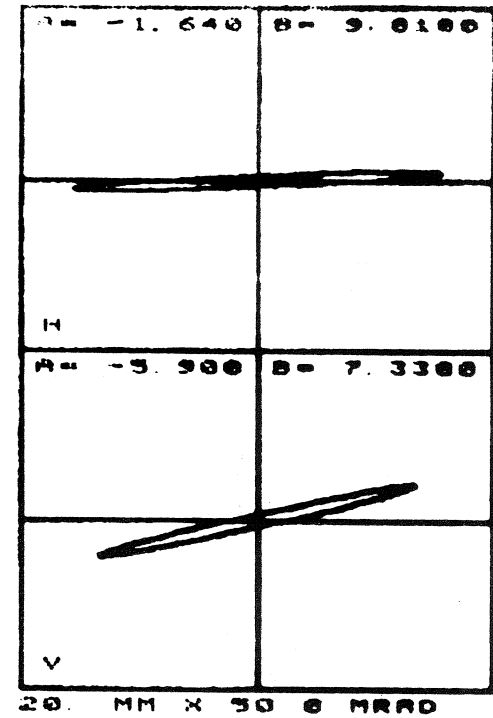
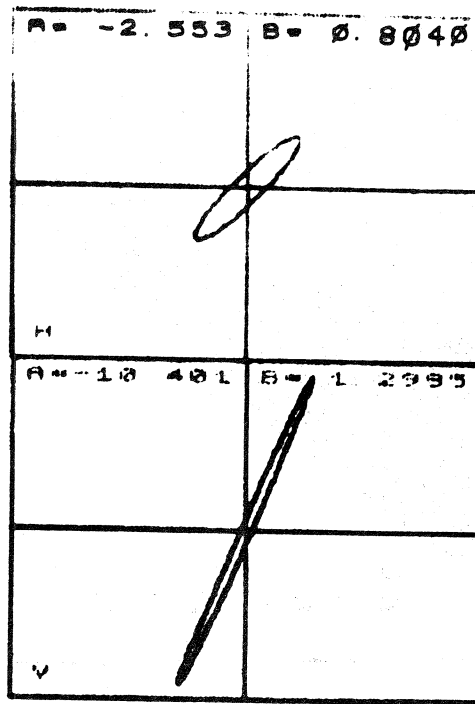
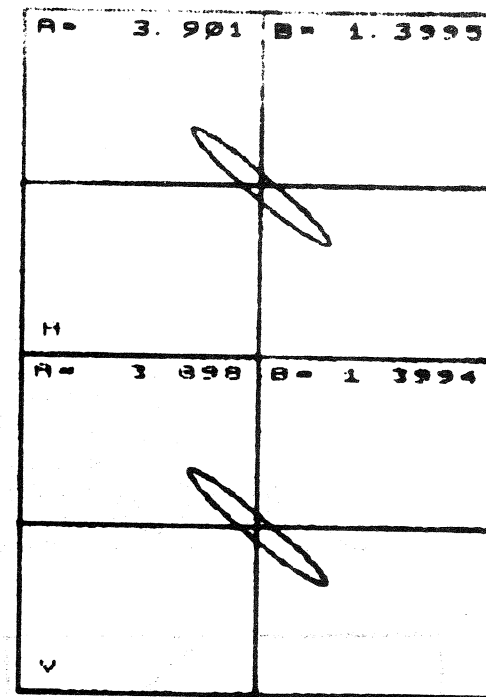


FIG. 18: Transfer of emittances as under Fig.17, but with changed values of outer quads of T2 and T3 (by +2.5%)



I = 90
EX = 25
EY = 25

NE	NP	VALUE
2	1	223 700
2	4	-237 010
7	1	-190 512
7	4	190 657



20 MM X 50 0 MRAD

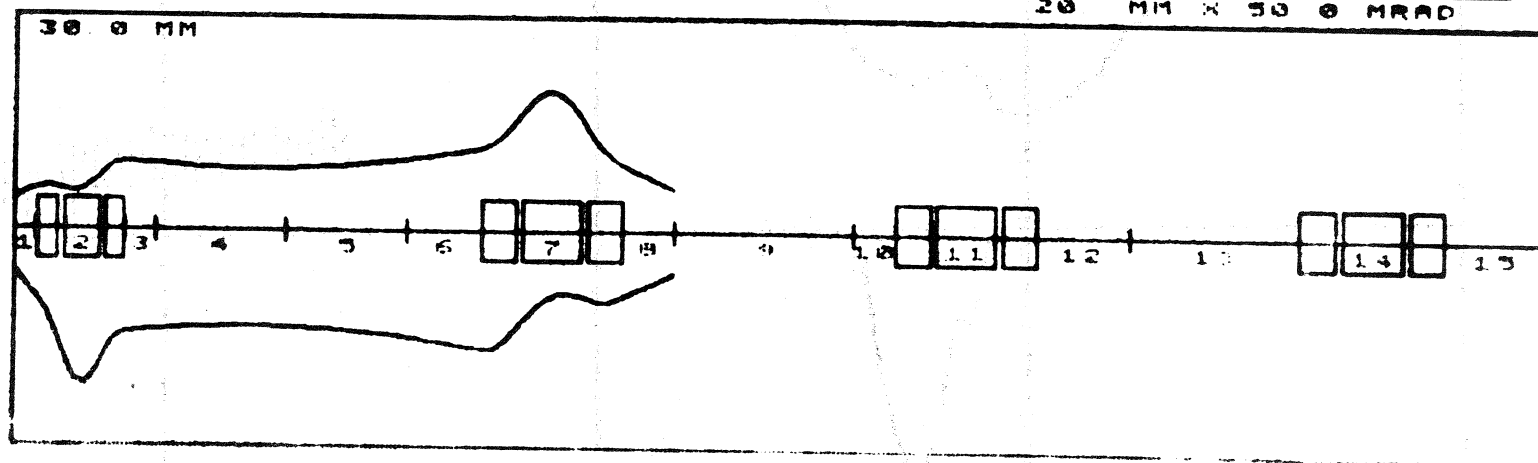
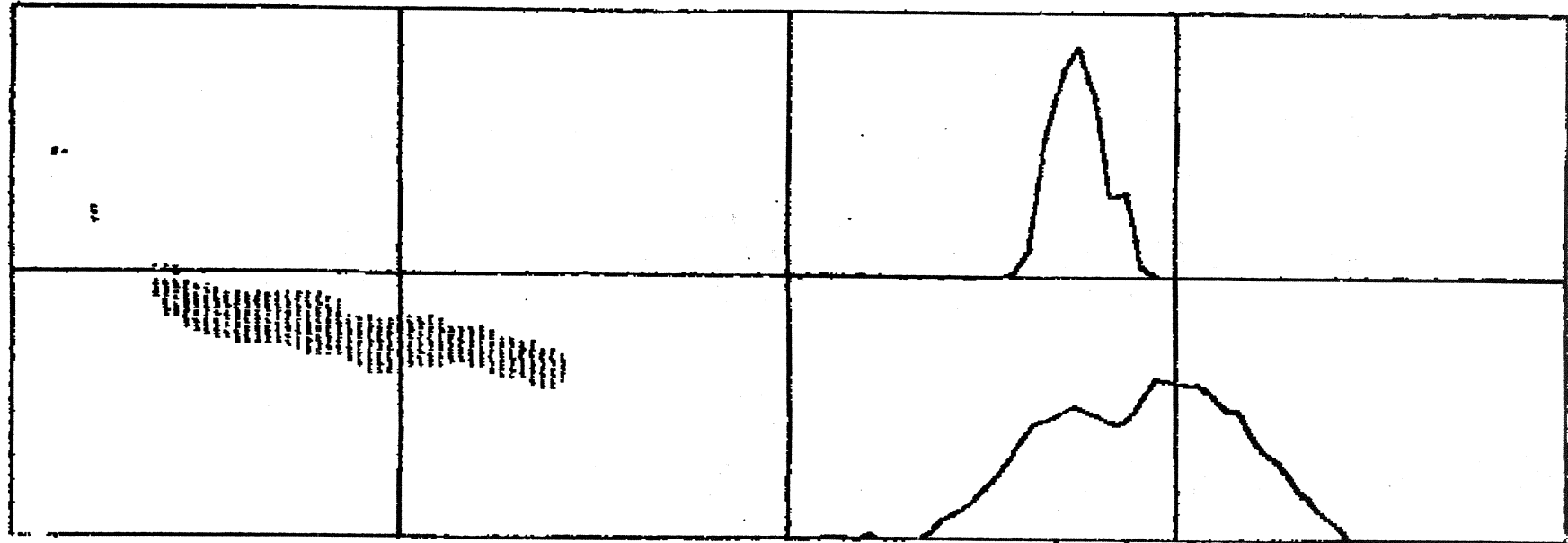


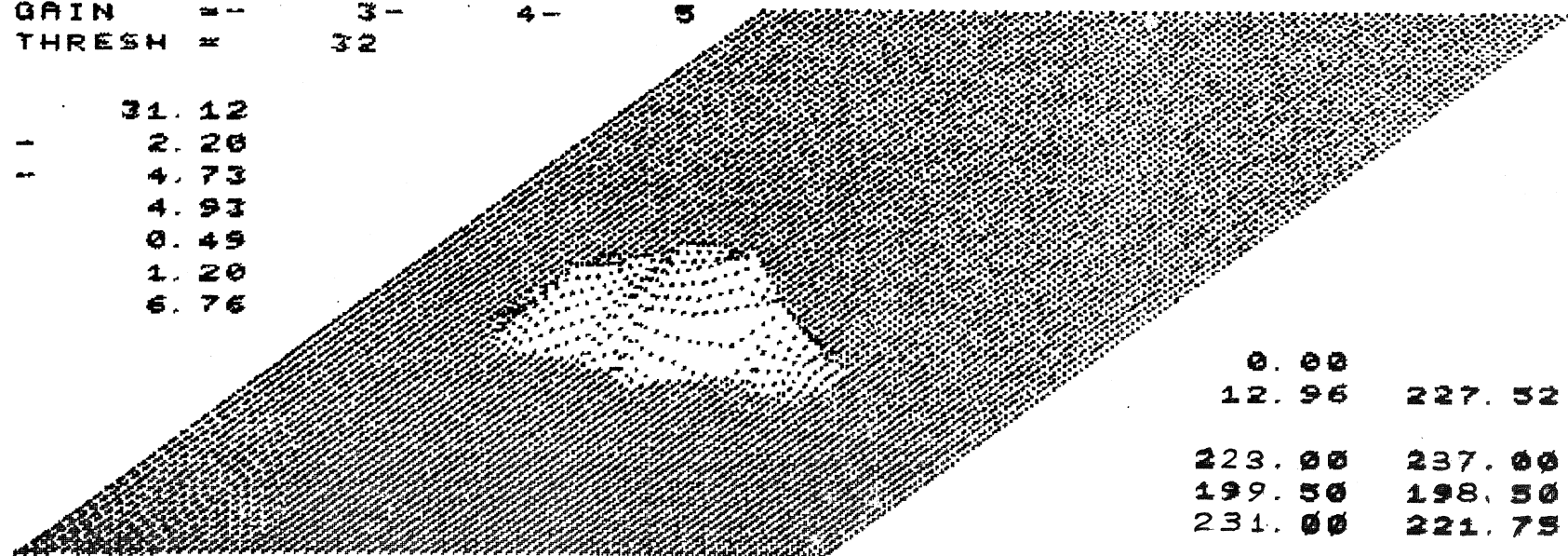
FIG. 19: Matching from LEBT input to AP1

750 KEY EMITTANCE MEASUREMENT - EM2 H - DATE: 77- 6-17



EM1310. W48. 1
 (47.5* 41.7) 23.7 133.5
 GAIN = 4 - 4 - 8
 THRESH # 32

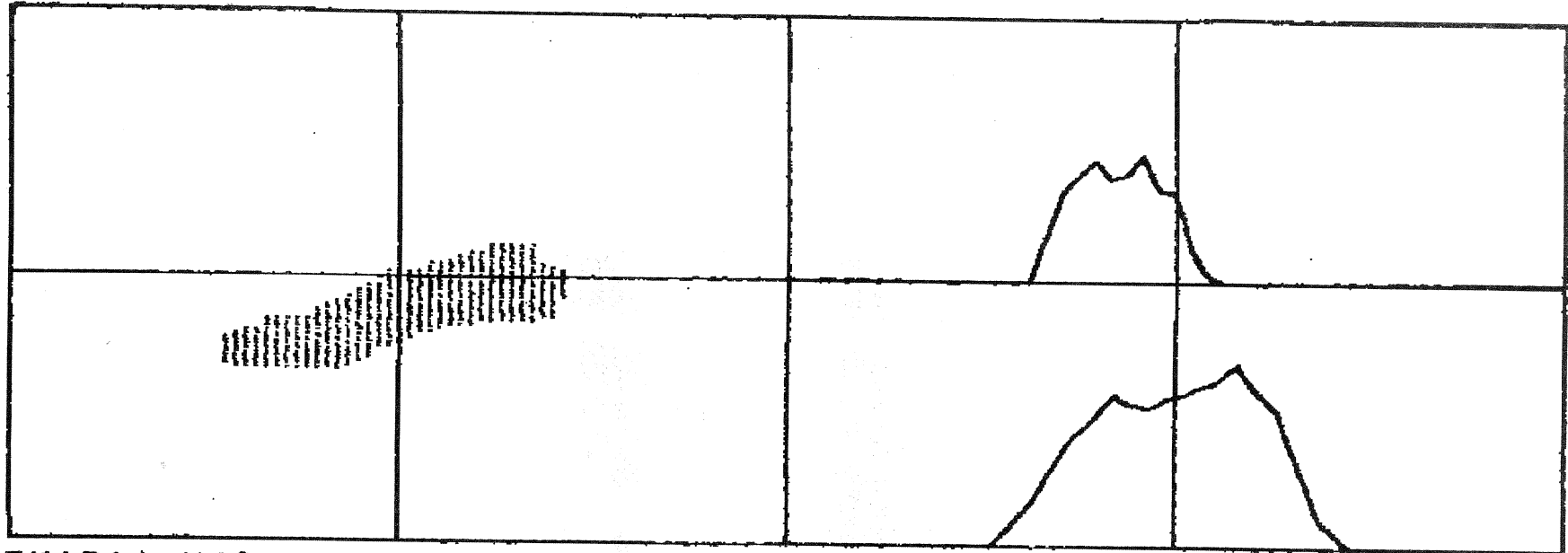
31.12
 2.26
 4.73
 4.93
 0.45
 1.20
 6.76



0.00
 12.96 227.52
 223.00 237.00
 199.50 198.50
 231.00 221.75

FIG. 20a: Measured horizontal beam emittance (at EM2) with new settings of T1 and T2

750 KEY EMITTANCE MEASUREMENT - EM2 V - DATE: 77- 6-17



EM1211. W48, 1
 (47.5 * 41.7) 23.7 133.8
 GAIN 1 - 4 - 4 - 8
 THRESH 1 - 4 - 4 - 8

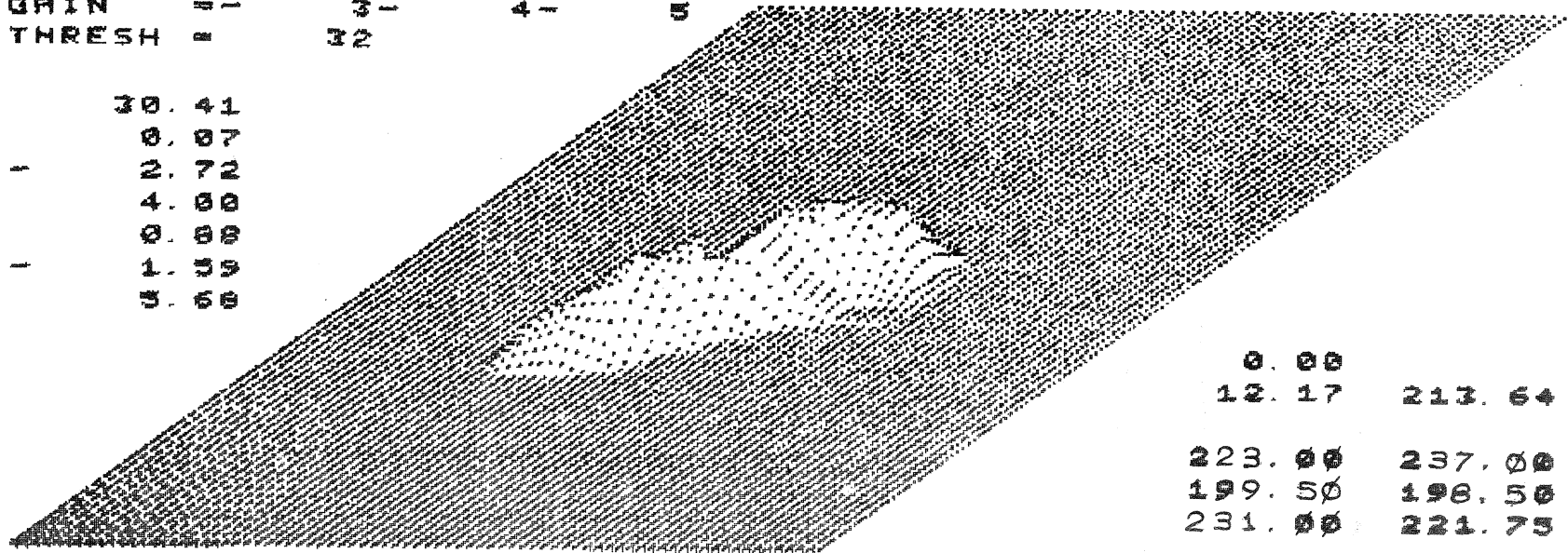
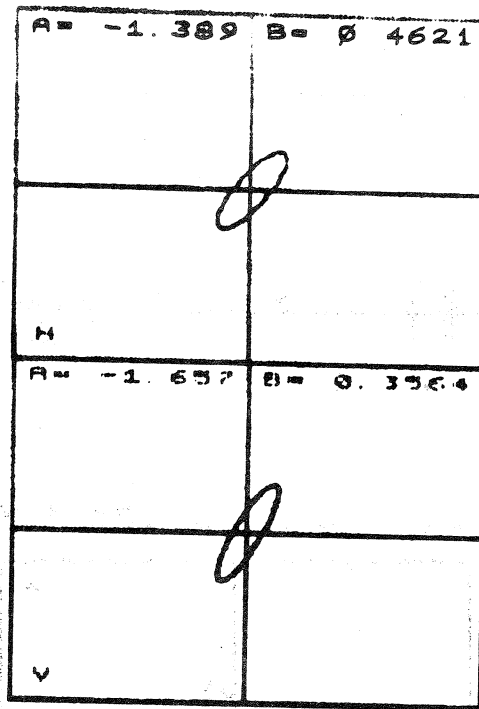


FIG. 20b: Measured vertical beam emittance (at EM2) with new settings of T1 and T2



I = 30
EX = 20
EY = 20

NE	NP	VALUE
11	1	231 500
11	4	-221 750
14	1	-160 000
14	4	154 000

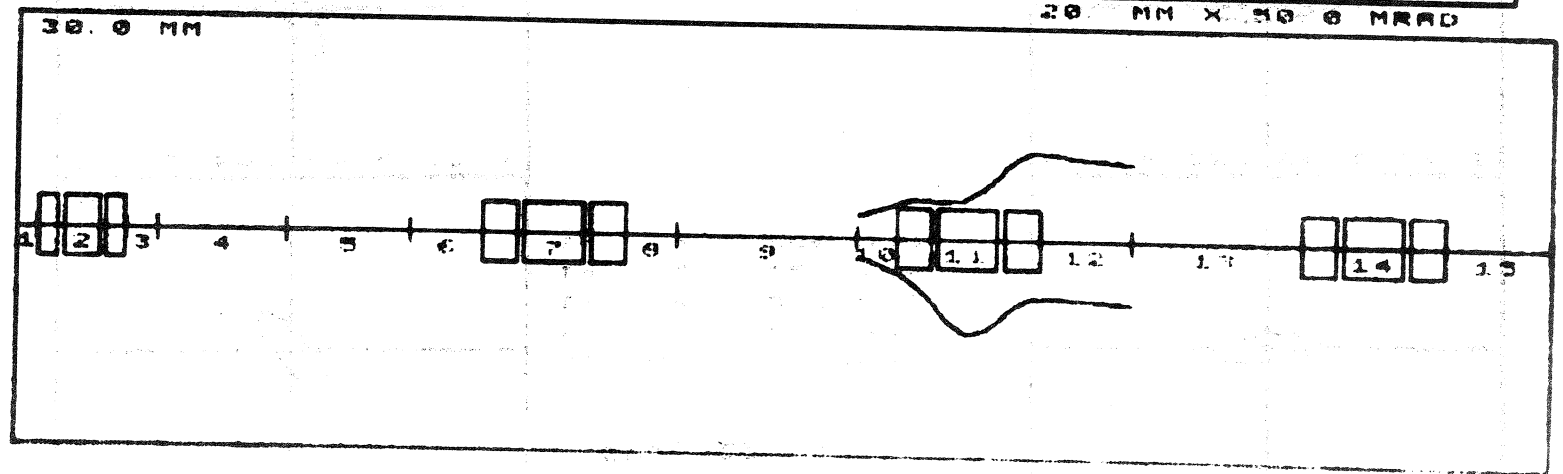
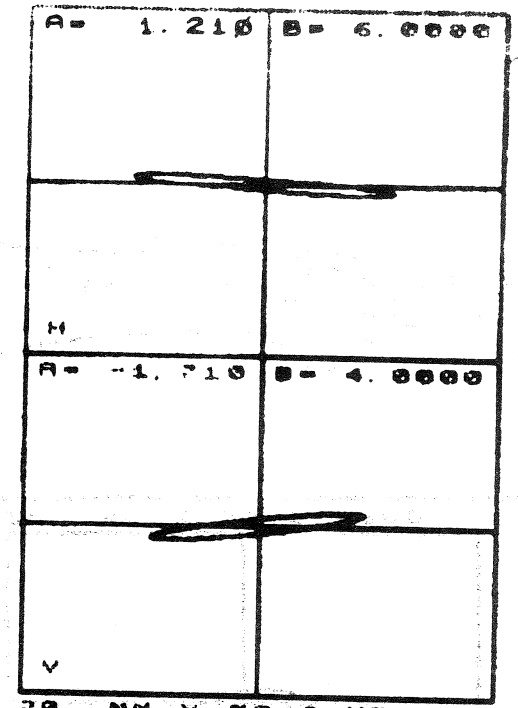
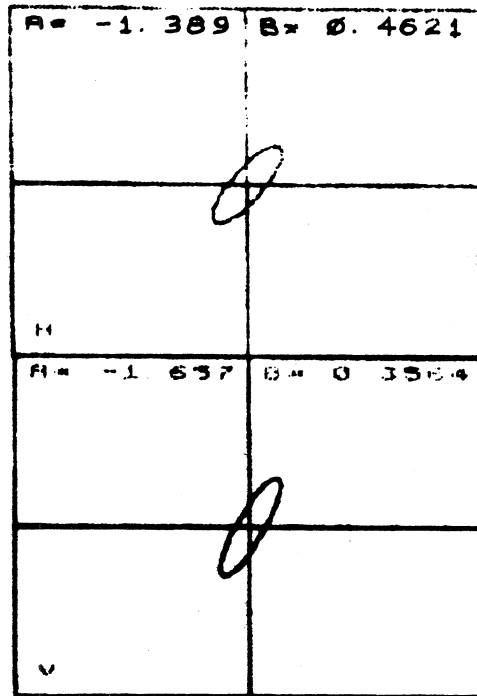
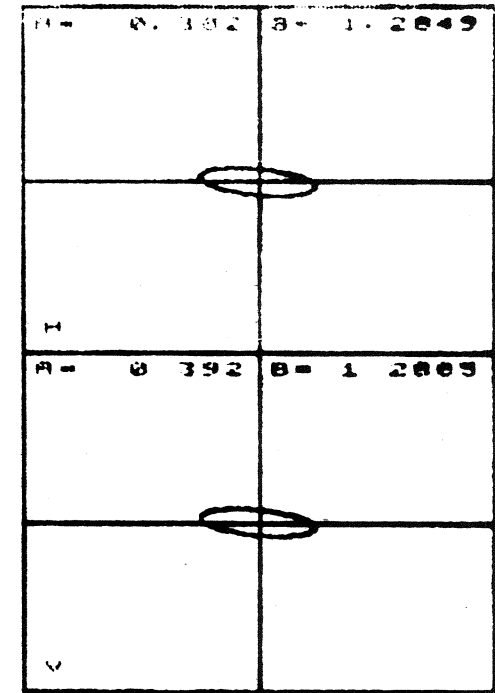


FIG. 21: Transfer of measured emittances (shown in Fig. 20) to T3 input



I = 90
EX = 20
EY = 20

NE	NI	VALUE
11	1	265 983
11	4	-245 001
14	1	-220 076
14	4	206 970



20 MM X 50 0 MRAD

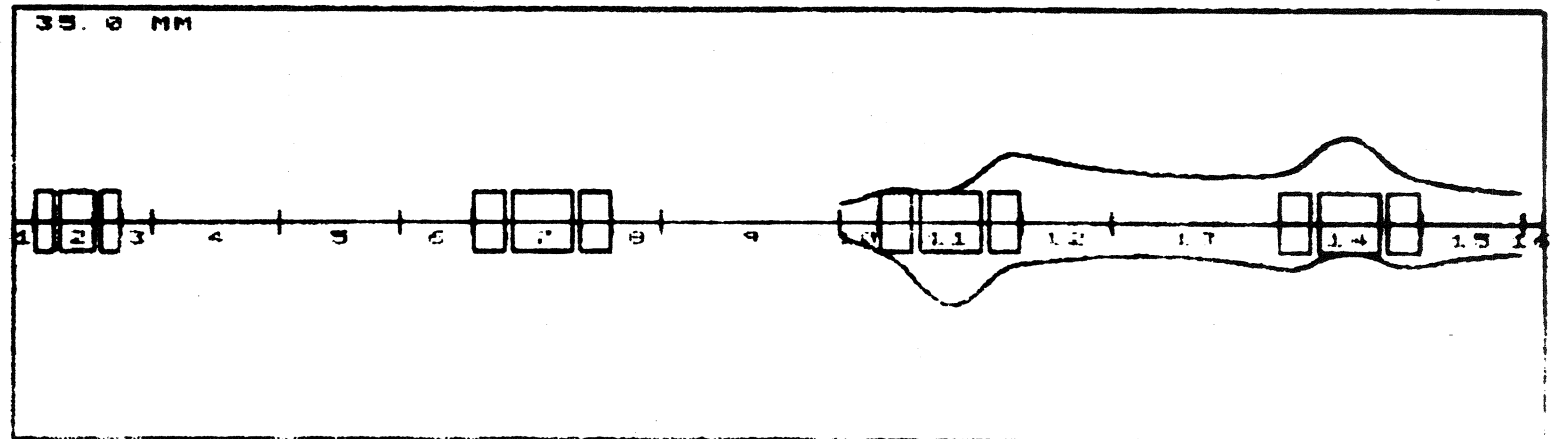
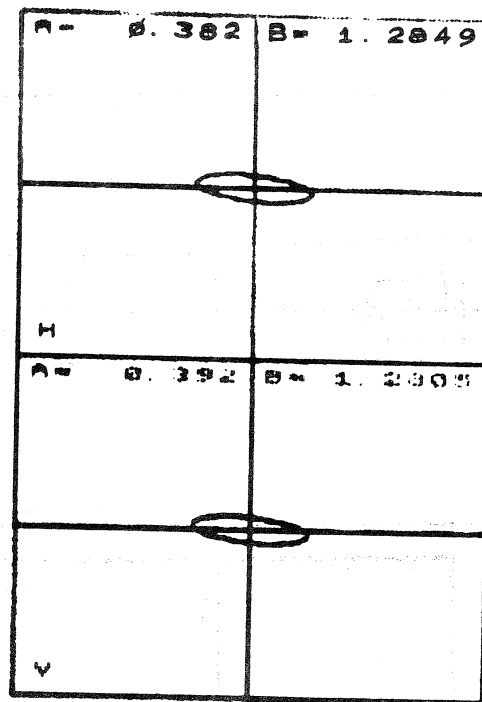


FIG. 22: Matching between T3 and the buncher DDHB



I = 00
EX = 20
EY = 20

NR	NP	VALUE
2	1	7 000
5	1	-120 000
8	1	249 414
10	1	-297 116
12	1	300 339
13	1	-112 707

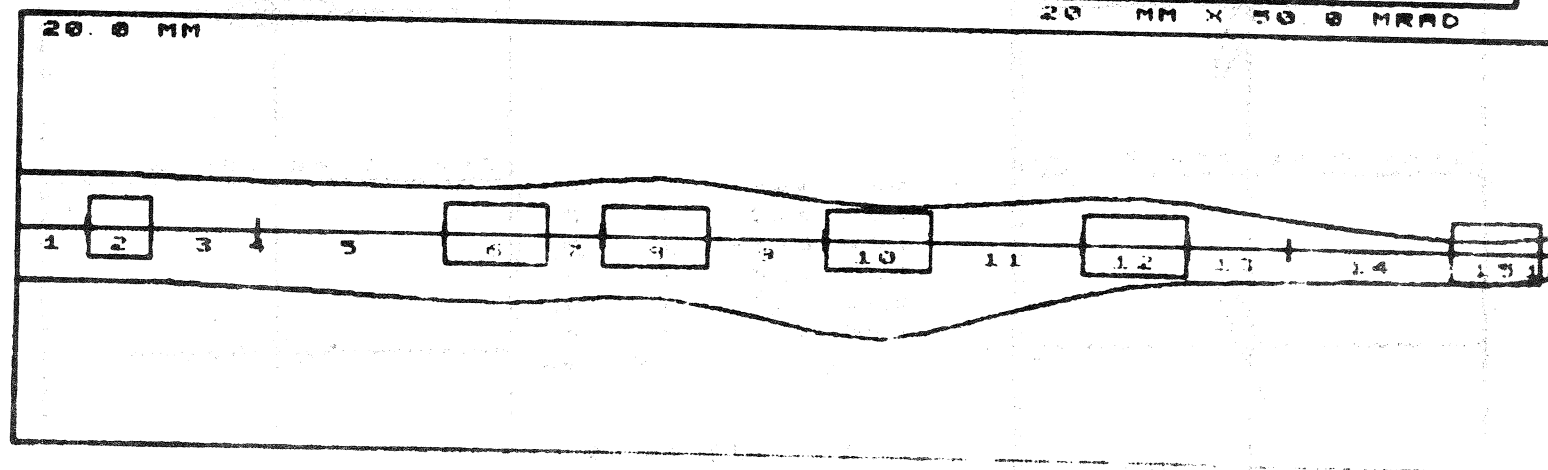
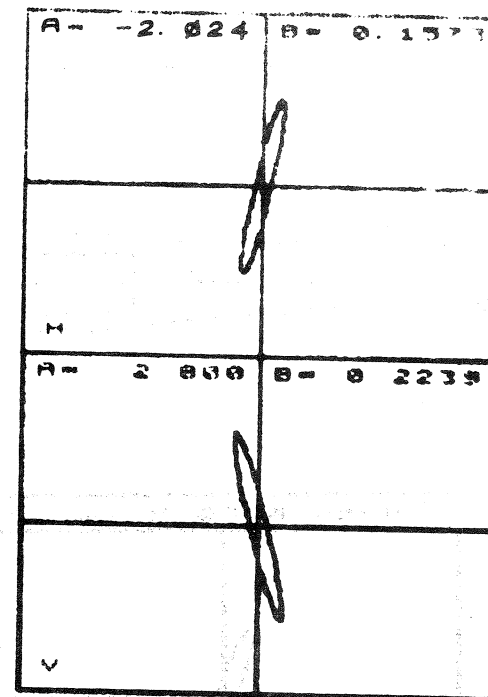
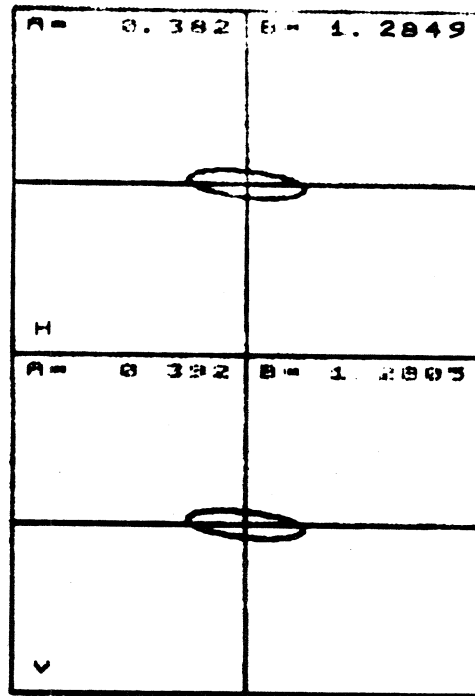
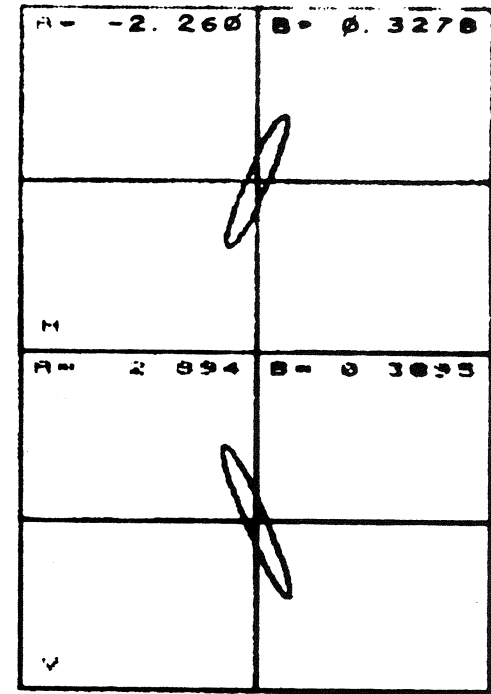


FIG. 23: Matching of unbunched beam from DDHB to Linac input



I = 80 204
 EX = 20 20
 EY = 20 21

NE	NP	VALUE
2	1	0.380
6	1	-1.270
8	1	2.250
10	1	-1.302
12	1	2.354
14	1	-1.81



20 MM X 50 ° MRAD

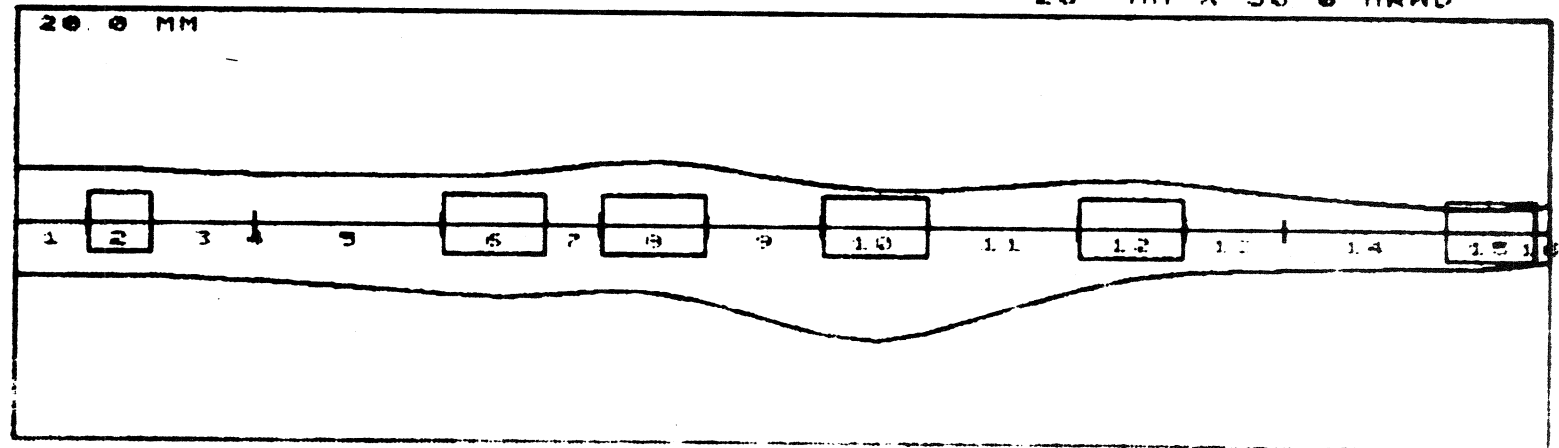
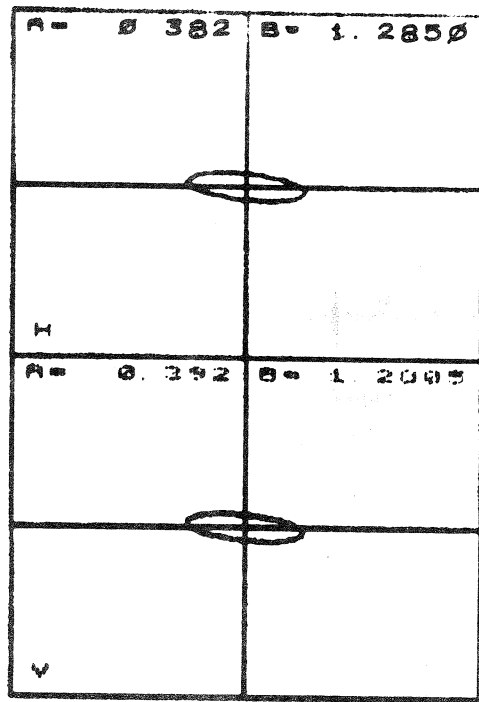


FIG. 24: Matching of bunched beam (only B1 operating) to Linac input



I = 80 304
 EX = 20 23
 EY = 20 26

NE	NP	VALUE
2	1	0.980
5	1	-1.120 0.000
8	1	2.554 0.078
10	1	-1.002 1.135
12	1	2.722 0.022
15	1	-1.920 0.071

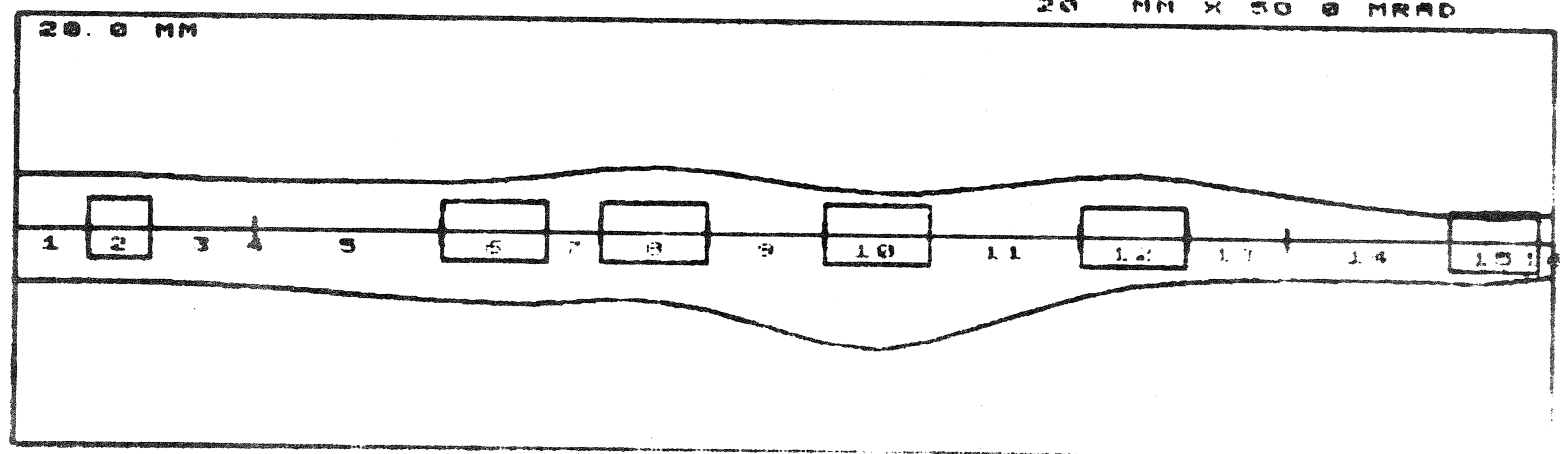
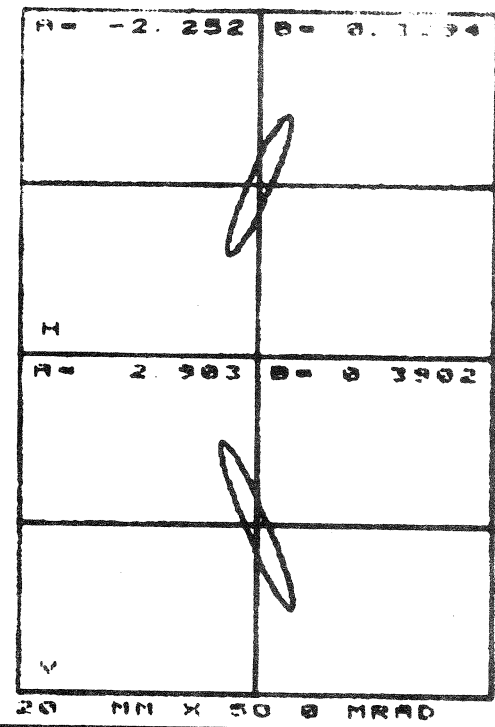


FIG. 25: Matching of bunched beam (B1 and B2 operating) to Linac input

